LLNL-TR-415215

LAWRENCE
LIVERMORE
NATIONAL
LABORATORY

Injection and Reservoir Hazard Management: The Role of Injection-Induced Mechanical Deformation and Geochemical Alteration at In Salah CO2 Storage Project: Status ReportQuarter end, June 2009

Joseph P. Morris, Walt W. McNab, Susan K. Carroll, Yue Hao, William Foxall, Jeffrey L. Wagoner

July 31, 2009

This work performed under the auspices of the U.S. Department of Energy by Lawrence Livermore National Laboratory under Contract DE-AC52-07NA27344.

Status Report
Quarter end, June 2009

Injection and Reservoir Hazard Management: The Role of Injection-Induced Mechanical Deformation and Geochemical Alteration at In Salah CO_2 Storage Project

WORK PERFORMED UNDER AGREEMENT

LLNL – FEW0149

SUBMITTED BY

Lawrence Livermore National Laboratory
7000 East Ave.
Livermore, California 94551

PRINCIPAL INVESTIGATOR

Joseph Morris
(925) 424-4581
(925) 422-3118
morris50@llnl.gov

SUBMITTED TO

U. S. Department of Energy
National Energy Technology Laboratory

Karen Cohen
cohen@netl.doe.gov

Auspices Statement
This work performed under the auspices of the U.S. Department of Energy by Lawrence Livermore National Laboratory under Contract DE-AC52-07NA27344.

1. EXECUTIVE SUMMARY

The In Salah Gas Project (ISG), a joint venture (JV) of BP, Sonatrach, and StatoilHydro, has two fundamental goals: (1) 25-30 years of 9 bcfy natural gas production from 8 fields in the Algerian Central Sahara, and (2) successful minimization of the associated environmental footprint by capture and subsurface isolation of the excess CO_2 extracted from production streams and subsurface isolation in the Krechba sandstone reservoir. The In Salah project provides an opportunity to study key physical and chemical processes in operational deployment of geological carbon sequestration. The objectives of the research are to study two components relevant to storage effectiveness and operational success at In Salah: Reactive chemistry of the brine-CO2-reservoir-caprock-wellbore system, and the geomechanical effects of large-scale injection on crustal deformation and fault leakage hazards. Results from this work will enhance predictive capability of field performance, provide a new basis for interpretation of geophysical monitoring at In Salah, and provide additional information relevant to the creation of geological sequestration standards. The Joint Industry Partners (JIP: BP, StatoilHydro, Sonatrach) and LLNL will share data and results to achieve the objectives of the proposed work.

The objective of the work performed at LLNL is to integrate LLNL core strengths in geochemistry and geomechanics to better understand and predict the fate of injected CO_2 in the field. The mechanical, chemical and transport properties of the reservoir-caprock system are coupled. We are using LLNL-developed quantitative tools to assess the potential for CO2 migration / leakage caused by injection-induced deformation. The geomechanical work is focused upon fault activation, fluid induced fracturing of the caprock and permeability field evolution of the fractured reservoir. These results will be used in concert with reactive transport calculations to predict the ultimate fate of the CO_2. We will integrate laboratory and reactive transport modeling to assess CO_2 plume migration and partitioning between different trapping mechanisms. Geochemical reactive transport modeling will be used to address multiphase flow (supercritical CO_2 and water), CO_2 dissolution, mineral sequestration, and porosity/permeability changes. The reactive transport portion of the work ultimately couples with geomechanical modeling. In particular, the distribution of the pressure perturbation induced by injection drives the geomechanical response. Subsequently, the geochemical work determines if water-rock interactions eventually enhance or suppress fractures.

A key focus of this work is to establish the site specific interactions of geomechanics, reactive flow and transport. This involves building and refining models of the reservoir and overburden. The models will undergo continual refinement in response to data collected in the field and experiments performed at LLNL and elsewhere.

This project commenced in FY08, with DOE funding starting in April, FY08. We have successfully initiated a cross-disciplinary study of the In Salah CO_2 sequestration project and have met all FY08 and FY09 Q1, Q2 and Q3 milestones. During the reporting period, we continued to acquire and process data from the JIP to import into our own geomechanical and geochemical computational tools. The lab testing program continued using both locally formulated cements and field samples from Krechba.

The geomechanical studies indicate that pore fluid pressures induced by injection will lead to significant permeability enhancement of the combination of fracture network and fault network within the reservoir in the vicinity of the injectors. We continued reactive

transport calculations for CO_2 rich fluids flowing through fractures. These calculations demonstrate that although porosity and permeability changes are expected in response to CO_2 injection they are not anticipated to have a significant effect upon transport properties within the reservoir or caprock. The experimental program continued on schedule, providing refined estimates of the in situ quality of the wellbore cement composition in the field. These results will be used to inform estimates of the risk of wellbore seepage of CO_2. Geomechanical analysis identified which faults are most likely flow conduits and which are expected to act as flow barriers for inclusion into reservoir models. Subsequent NUFT simulations were performed based upon this information and the results indicate that the presence of faults in the vicinity of the KB-502 injector may be responsible for the early breakthrough of CO_2 observed at KB-5. Additionally, we have simulated the uplift of the overburden resulting from NUFT reservoir models of fluid injection and compared the results with the InSAR data. By including conducting faults into our reservoir and overburden model we achieve better agreement with the observed net uplift at the ground surface, but not the shape of the observed uplift. However, by including flow into a *hypothetical* fault into the lower caprock, our simulations better match the morphology of the surface deformation observed via InSAR. Our results indicate that the best fit is obtained through a combination of reservoir and fault pressurization (rather than either alone).

2.Statement of Project Objectives

OBJECTIVES

The In Salah Gas Project (ISG), a joint venture (JV) of BP, Sonatrach, and StatoilHydro, has two fundamental goals: (1) 25-30 years of 9 bcfy natural gas production from 8 fields in the Algerian Central Sahara, and (2) successful minimization of the associated environmental footprint by capture and subsurface isolation of the excess CO_2 extracted from production streams and subsurface isolation in the Krechba sandstone reservoir. The In Salah project provides an opportunity to study key physical and chemical processes in operational deployment of geological carbon sequestration. The objectives of the research are to study two components relevant to storage effectiveness and operational success at In Salah: reactive chemistry of the brine-CO_2-reservoir-caprock-wellbore system, and the geomechanical effects of large-scale injection on crustal deformation and fault leakage hazards. Results from this work will enhance predictive capability of field performance, provide a new basis for interpretation of geophysical monitoring at In Salah, and provide additional information relevant to the creation of geological sequestration standards. The Joint Industry Partners (JIP: BP, StatoilHydro, Sonatrach) and LLNL will share data and results to achieve the objectives of the proposed work.

SCOPE OF WORK

This study is composed of a comprehensive multi-disciplinary effort that addresses two fundamental challenges to successful geologic CO_2 isolation at In Salah that are equally relevant to the broad range of CO_2 storage scenarios:

1) Quantify CO_2 plume migration and sequestration partitioning among distinct trapping mechanisms within dynamic, complex permeability fields characterized by multi-scale heterogeneity—emphasizing assessment of coupled processes that may lead to early CO_2 breakthrough at production wells.
2) Evaluate geomechanical response and potential supra-reservoir leakage, through faults, fractures and well bores, which may ultimately reach the surface.

The objectives of the study will be accomplished by completing the following activities:

- Construction of reactive transport and geomechanical models
- Batch/mixed flow reactor experiments and modeling
- Plug-flow reactor experiments and modeling
- Field-scale reactive transport modeling
- Fault failure forecasting
- Discrete fracture modeling
- Simulation of microseismicity

Successfully addressing these challenges requires quantitatively representing injection-triggered hydraulic, geochemical and mechanical processes within reservoir, caprock, and well-bore environments. Such representation requires modeling approaches that explicitly integrate these processes. The proposed research will augment and advance ISP's earlier in-house reservoir simulation work by adding explicit account of permeability evolution due to injection-triggered geomechanical and geochemical processes, which together may lead to significant modification—enhancement or degradation—of reservoir, caprock, and well-bore integrity. Specifically, dynamic pressure perturbations may cause rapid aperture modification of pre-existing faults and fractures through mechanical deformation, while imposed chemical disequilibria may cause concomitant, yet kinetically retarded, aperture modification through fluid-rock mass transfer and dependent volume alteration of bounding matrix blocks. Understanding and quantifying this complex interaction of geomechanical and geochemical contributions to permeability evolution lies at the heart of developing computational capabilities that accurately forecast the long-term isolation performance of CO_2 storage sites.

TASKS TO BE PERFORMED

Our research plan includes reactive transport and geomechanical modeling over a range of scales and builds upon systematic experimentation. We will employ a set of LLNL-developed computational tools well suited to these problems.

Task 1.0 – In Salah Storage Project Data Acquisition, Interpretation, and Information Exchange

Predictive modeling efforts rely on accurate characterization of the subsurface environment. This component of our research will involve obtaining/interpreting available data from BP and ISP relating to the geochemical, mechanical and hydrologic properties of the reservoir, caprock and overburden. These data will provide a framework for our subsequent experimental and modeling efforts.

Subtask 1.1 Data Acquisition

BP has provided provisional agreement to share various kinds of data with LLNL to execute the tasks discussed above (see below). These data will be provided at the earliest availability in order to give investigators sufficient time to meet key milestones and deliverables. BP will maintain propriety over release and sharing of primary data and BP prior models. Data derived from new simulations of these models will be owned by LLNL, but for a period of 2 years after generation of new derived data and results publication of these data will require formal BP approval.

Critical information required for predictive geomechanical modeling includes the following:

- Orientation and magnitude of the in-situ stress tensor
- 3D fault geometry as interpreted from seismic data and well logs
- Orientation and estimated densities/apertures of pre-existing and drilling-induced fractures
- Reservoir and caprock mechanical constitutive properties
- 3D velocity model
- Structural history
- Waveforms, locations, and source moments from injection-induced micro seismic events

For reactive transport modeling, the preceding list must be augmented to include (ideally) all of the following:

- Porosity/permeability ranges and their degree/style of heterogeneity
- Detailed mineralogy/petrography, including trace silicates/oxides/sulfides, solid-solution compositions (e.g., for clays), cementation characteristics, etc.
- Detailed chemical analyses of the reservoir aqueous phase (major/trace elements)
- Sampling locations for the above data (obtained from core and fluid samples)
- Current pressure-temperature conditions
- CO_2 influx parameters: projected rates, duration, and injection well locations
- CO_2 compositional parameters: impurity concentrations
- Local and regional hydrologic flow gradients
- Capillary entry pressure data for caprock lithologies
- Core samples from the reservoir and caprock for experimental/modeling studies
- Geophysical monitoring data that may delineate plume geometry as a function of time

- Residual CO_2 saturations that characterize the Krechba reservoir
- Location of the initial and current CH_4-water contact

Subtask 1.2 Data Interpretation

We will use the data supplied by BP and ISP to construct numerical models of the reservoir, caprock, and overburden. Critical components of this process will include incorporating geological structure and heterogeneity into our models and developing boundary and initial conditions that are representative of field conditions. These models will form the basis for our reactive transport and mechanical deformation simulations detailed below.

Subtask 1.3 In Salah Operator Information Exchange

Throughout the duration of the project, we will continue to exchange results and data with BP and ISP. This ongoing communication will facilitate refinement of our models and provide insights to BP and ISP regarding future data acquisition.

Task 2.0 Reactive Transport Studies

Our reactive transport studies will combine modeling and experimental components to provide improved predictions of CO_2 plume migration, permeability evolution, and isolation performance at In Salah. Our approach is two-fold: (1) conduct and model batch, mixed-flow, and plug-flow reactor experiments using representative reservoir and caprock samples, and (2) carry out field-scale 2- and 3-D reactive transport simulations of CO_2 injection into the Krechba reservoir. The proposed research builds upon and extends our Sleipner modeling studies (Johnson et al., 2004a) and CCP-I work on simulating long-term caprock integrity (Johnson et al., 2005a); it also leverages our Frio work (Knauss et al., 2005; Kharaka et al., 2006) and experience conducting integrated modeling/ experimental studies (Johnson et al., 1998, 2005b).

Subtask 2.1 Batch/mixed flow reactor studies

These analyses are designed to assess CO_2-dependent chemical and porosity/permeability evolution (1) in the vicinity of the reservoir/caprock interface, and (2) within both the reservoir and caprock. . For investigating the reservoir/caprock interface, the sample chamber will contain crushed reservoir and caprock material; for investigating completion cement, it will contain an inner cylindrical core of fresh cement surrounded by either crushed Krechba reservoir or caprock material. For both sets of batch and mixed-flow experiments, the chamber will initially be filled with CO_2-saturated brine at field P-T conditions. In the batch (closed system) runs, this initial condition will be allowed to steep over an appropriate time frame; in contrast, the mixed-flow (open system) runs will be characterized by continuous fluid stirring (to minimize compositional gradients), influx, and withdrawal at controlled rates. Thus, the batch experiments represent diffusion-dominated reaction progress (no advective fluid flow; i.e., relatively minimal chemical/permeability evolution), while the mixed-flow experiments represent advection-dominated reaction progress (continuous fluid flow; i.e., relatively maximal evolution). In all of these experiments, fluid chemistry will be sampled during the runs and mineral alteration products will be sampled and analyzed post-mortem. Agreement between measured and predicted chemical and permeability evolution will be optimized by fine-tuning key thermodynamic, kinetic, and hydrologic parameters within uncertainty limits.

Subtask 2.2 Plug-flow reactor studies

This analysis is designed to assess CO_2-dependent chemical evolution along the cement/reservoir, cement/caprock, and reservoir/caprock interfaces as well as permeability evolution within the reservoir and caprock damage zones. The sample chamber will be configured such that one longitudinal half (parallel to flow) is occupied by representative cement and the other is divided into equal-parts crushed Krechba reservoir and caprock material. Metered flow of CO_2-saturated brine will be restricted to the crushed-material half and therefore will interact with cement only along its interfaces with sandstone and shale. This set-up represents a physical analog to the cement contact with reservoir and caprock damage zones; hence, it provides a forum for evaluating chemical evolution that attends advective flow of carbonated brine through these zones as well as its diffusive migration into cement. Data collected to assess such evolution will include time-dependent effluent fluid compositions as well as post-mortem mineralogical and petrographic analyses of cement, sandstone, and shale. Real-time permeability evolution of the sandstone/shale half will be retrieved from data recorded by the differential pressure transducer. Experimental P-T conditions will approximate those of the reservoir/caprock interface at Krechba. Agreement between measured and predicted chemical and permeability evolution will be optimized by fine-tuning key thermodynamic, kinetic, and hydrologic parameters within uncertainty limits.

Subtask 2.3 Field-scale integrated reactive transport and geomechanical studies

Grounded by the preceding work, two sets of field-scale reactive transport simulations will be carried out, each spanning both active-injection and post-abandonment phases of the isolation process. The first set will address plume migration, sequestration partitioning among distinct hydrodynamic, solubility, and mineral trapping mechanisms, and permeability evolution. Here, the focus will be on quantifying the effects of geochemical and geomechanical processes unconsidered within earlier ISP in-house reservoir simulation efforts. Particularly important are their potential impacts on plume arrival time at the gas accumulation, reservoir injectivity, storage capacity, and caprock seal integrity. To the extent feasible (from both technical and proprietary standpoints), 2- and 3-D simulation domains will be consistent with—and possibly extracted directly from—the same site geologic model used in ISP's earlier in-house reservoir simulation work; i.e., our EarthVision/NUFT interface will be used to translate detailed lithologic heterogeneity directly from the site geologic model into NUFT spatial domains.

In this first set of simulations, the effect of geomechanical processes on reservoir/caprock permeability evolution will be assessed using the unidirectional NUFT/LDEC interface developed under CCP-1 (Johnson et al., 2005a), which translates injection-triggered pressure history into the corresponding effective stress and fracture aperture evolution. This translation will be carried out under the Geochemical modeling task "caprock deformation and fracture", as described below. At present, this geomechanical evolution (LDEC) is not back-coupled into the multiphase flow and reactive transport model (NUFT); i.e., the dependence of permeability, fluid flow, and pressure history on concomitant geomechanical aperture evolution is not represented. As a result, the magnitudes of predicted pressure increase and aperture widening represent upper-limit values, which provide the most critical bound on anticipated performance.

The second set of simulations will address potential CO_2 migration within the localized well-bore environment. In these models, particular attention will be paid to capturing the observed radial extent and pre-injection permeability enhancement of reservoir and caprock well-bore damage zones. The focus will be on quantifying long-term chemical and permeability evolution within these zones, along cement/reservoir and cement/caprock interfaces, and within the cement itself. Particularly significant is potential leakage through gas production well-bore environments, which will ultimately be exposed to the replacement CO_2 accumulation.

Task 3.0 Geomechanical Studies

Fractures and faults are expected to play an important role in plume migration within the reservoir and provide potential pathways for leakage of CO_2 from the reservoir. We will develop discrete fracture network models that are representative of: 1) the known structural geometry of major faults and fractures in and above the reservoir and 2) conceptual models of caprock structure. With these discrete fracture models, we will use LLNL's proprietary LDEC code (Morris et al., 2003; Johnson et al., 2004, 2005a) to calculate fluid-pressure driven deformations of the fractured rock mass at different scales. LDEC can be used to simulate normal and/or shear deformation along individual fractures or faults as well as networks of fractures with arbitrary orientation, length, and mechanical properties. All of the elements (rock blocks) can deform independently potentially resulting in slip and/or dilation of existing fractures due to changing pore pressures. Coupling LDEC with a recently developed discrete-fracture-network flow code (FracHMC) that accommodates stress-induced changes in transmissivity (Detwiler et al., 2006) will provide estimates of changes in effective permeability caused by altered transmissivities of individual fractures within the fracture networks.

Subtask 3.1 Fault/fracture studies

Given the geometry of major faults and fractures in and above the reservoir and estimates of the in-situ stresses, we will use LDEC to forecast the minimum change in effective stress needed to induce slip along portions of the fault (e.g., Wiprut and Zoback, 2002; Chiaramonte et al., 2006). This will require populating the large-scale fracture network model with mechanical properties that are representative of the different formations within the reservoir and overburden. Then, incrementally increasing pore pressures within regions of the reservoir will eventually lead to slip along one or more of the faults in the system. Using this approach, we will develop estimates of failure pressures along fault elements within the reservoir. It is believed that such fault failure events lead to both induced seismicity and the potential for substantial fluid flow along the fault. This analysis will provide estimates of the magnitude of reservoir pressure perturbations likely to cause slip along major faults, resulting in a potentially major leakage pathway. In addition, LDEC simulations of fault slip will provide estimates of seismic source terms resulting from the slip events, which can then be propagated through the overburden (described below) to provide simulated seismic signals at the surface or in boreholes.

Injection-induced increases in pore pressure lead to reservoir expansion and deformation of the caprock, which in turn may cause new and/or pre-existing fractures to open by induced tensile (Mode I) or shear stresses (Modes II and III). Furthermore, induced strain along weak discontinuities, such as fractures or bedding planes within the caprock can damage well-bore cements and casing. We will quantify the potential significance of these compromises to seal integrity at In Salah by using LDEC to predict the evolution of fracture apertures that corresponds to that of pore fluid pressure, as predicted by the field-scale reactive-transport modeling task, described above. The distribution and transmissivity of fractures that are created and/or opened by injection-imposed stresses will provide quantitative estimates long-term CO_2 leakage from the reservoir. In addition, a first-order quantitative assessment of aperture evolution due to explicitly integrated geochemical and geomechanical components will be carried out as a fundamental project integration task (see below).

Subtask 3.2 Injection-induced seismicity studies

The outputs from LDEC described above also serve as the basis for seismic modeling. The orientation and magnitude of local stresses, and fracture orientations provide the initial conditions for modeling seismic events. Shear failures, induced by changing pore pressures, produce seismic events that provide source terms for predicting seismograms through wave propagation from the reservoir to the surface. LLNL has developed a new 3D wave propagation code, WPP, that runs much faster and with greater stability than prior codes (Petersson et al., 2006). We will model the failure events as seismic source terms and match the modeled wavefields with seismograms recorded at In Salah. This will provide a tool for inverting microseismic results to better interpret the relation between monitored events and the distribution of CO_2 and pressure at depth.

Task 4.0 Integration of Reactive Transport and Geomechanical Study Results for Field-scale Interpretation

Ultimate enhancement or degradation of reservoir, caprock, and well-bore integrity hinges on the relative impact and rates of concomitant geochemical and geomechanical contributions to permeability evolution in these environments. In lieu of fully (bi-directionally) coupled reactive transport and geomechanical modeling capabilities, we have developed an aperture-based conceptual framework that facilitates explicit integration of these components, which in turn permits first-order predictive assessment of ultimate permeability modification for any site-specific CO_2 injection scenario (Johnson et al., 2003, 2004). In this integration task, results from the field-scale reactive transport and caprock deformation modeling work will be dovetailed within this framework to estimate net permeability evolution due to predicted geochemical and geomechanical contributions at In Salah. The results from both the individual and integrated studies can contribute information to the development of field operational protocols, both in the context of the In Salah site but potentially for broader application internationally.

DELIVERABLES

The following deliverables will be provided:

- Project Management Plan (Due at the start of the FWP)
- Progress Reports (Due Quarterly and shall at a minimum document technical, cost, and schedule status)
- Yearly Topical Reports (Due yearly for FWPs with greater than 18 months duration)
- Conference Papers/Proceedings (A copy of any conference papers/proceedings are required to be submitted)
- Final Scientific/Technical Report (Due at the completion of the FWP, should be a comprehensive document covering all years of the FWP)

BRIEFINGS/TECHNICAL PRESENTATIONS

LLNL will prepare detailed briefings for presentation to the NETL Project Manager. Briefings will be given by LLNL to explain the plans, progress, and results of the technical effort.

3.Major Milestone Status
MILESTONE LOG

FY08 Milestone Descriptions	Schedule Request	Completion Date/achievement
A. Initiate design of new experimental reactor apparatus to study In Salah demonstration project reservoir, caprock, and well-bore integrity	12/31/07	MET. A kick-off meeting was held with LLNL investigators to discuss reactor design and reactive chemistry experiments.
B. Establish requirements for In Salah demonstration project data and information exchange through technical meeting with BP	3/31/08 New: 6/30/08	MET. A kick-off meeting was held at LLNL on 6/5/08 with BP/StatoilHydro to exchange data and discuss project goals.
C. Initiate construction of discrete fracture network model for In Salah demonstration project fault/fracture networks in reservoir and overburden	6/30/08	MET: An initial discrete fracture model has been developed using BP data
D. Initiate development of preliminary failure envelope calculations for In Salah demonstration project fault/fracture networks	9/30/08	MET: Initial simulations of fracture response to fluid injection have been performed.

FY09 Milestone Descriptions	Schedule Request	Completion Date/achievement
E. Provide progress update to BP of initial phase of geomechanical and geochemical analysis through technical meeting	12/31/08	MET. BP hosted a workshop on October 15-16, 2008 in London attended by key participants from the ISP and currently-funded researchers. LLNL discussed the status of their results to date and established working relationships with other groups.
F. Complete initial reactor studies of In Salah demonstration project well-bore cements	3/31/09	Met. The initial series of reactor studies have been completed. Results documented in this report.
G. Initiate integration of reactive transport and geomechanical study results for In Salah demonstration project fault/fracture networks	6/30/09	Met. We have simulated the geomechanical response of the overburden including fault to the predicted porepressure distribution from the reactive transport calculations
H. Initiate injection induced seismicity study for In Salah demonstration project	9/30/09	

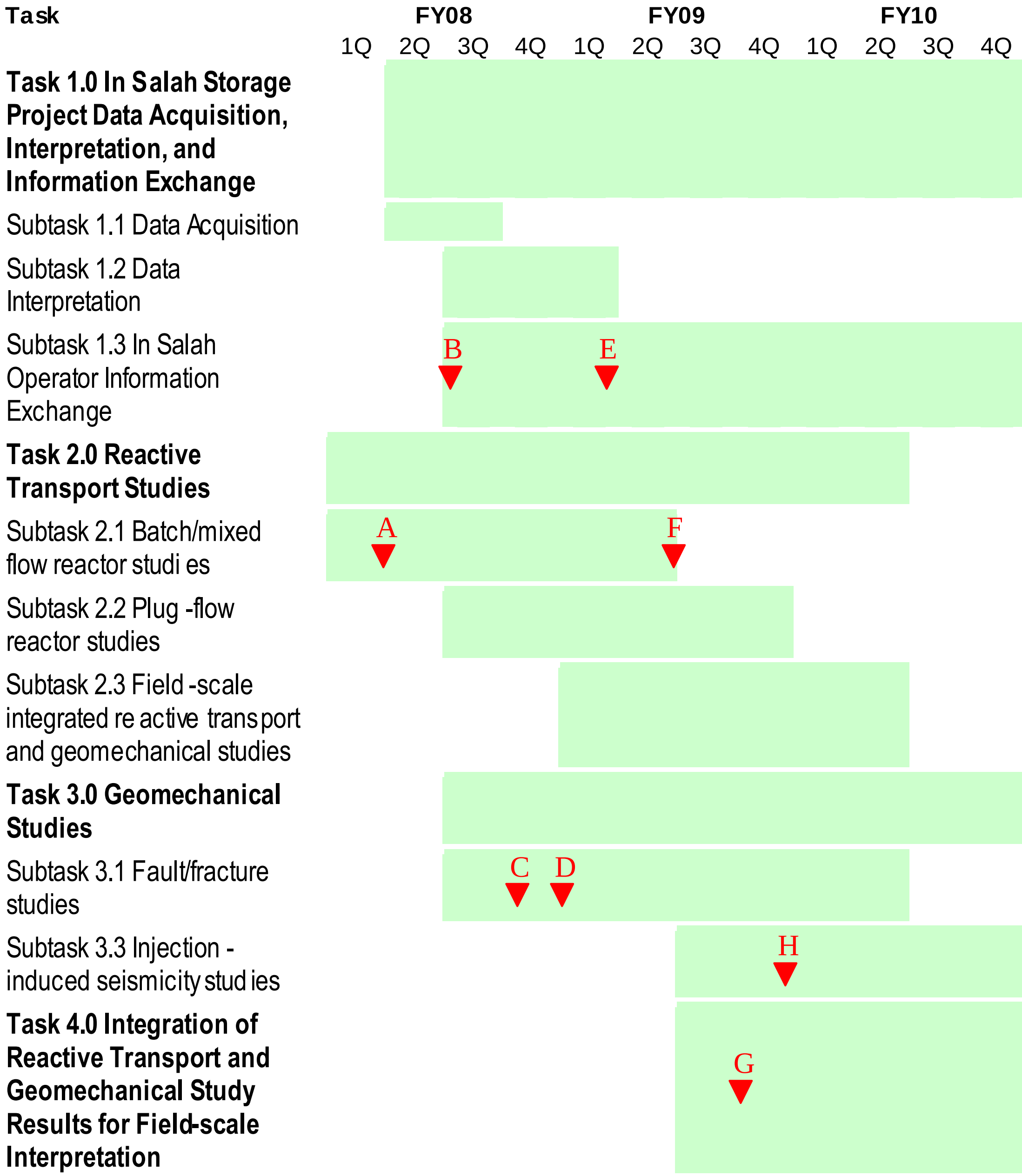
Task
FY08
FY09
FY10
1Q 2Q 3Q 4Q 1Q 2Q 3Q 4Q 1Q 2Q 3Q 4Q
Task 1.0 In Salah Storage Project Data Acquisition, Interpretation, and Information Exchange
Subtask 1.1 Data Acquisition
Subtask 1.2 Data Interpretation
Subtask 1.3 In Salah Operator Information Exchange
B
E
Task 2.0 Reactive Transport Studies
Subtask 2.1 Batch/mixed flow reactor studi es
A
F
Subtask 2.2 Plug -flow reactor studies
Subtask 2.3 Field -scale integrated re active transport and geomechanical studies
Task 3.0 Geomechanical Studies
Subtask 3.1 Fault/fracture studies
C
D
Subtask 3.3 Injection - induced seismicity stud ies
H
Task 4.0 Integration of Reactive Transport and Geomechanical Study Results for Field-scale Interpretation
G

4.Chronological Listing of Significant Events and Accomplishments

Significant Events

Date	**Description**
4/21-23/2009	Hosted workshop of ISP participants
5/2009	Received overburden model from JIP
6/17/2009	Telecon between LLNL and JIP

Accomplishments

Date	**Description**
4/2009	Extended NUFT reservoir model of KB-502/KB-5 area to include hypothetical flow into the lower caprock, and performed reservoir-scale multiphase flow simulations
5/2009	Simulated the geomechanical response of the overburden including fault to the predicted pore pressure distribution from the reactive transport calculations
6/2009	Commenced LDEC simulations of hydromechanical response of overburden to pressurization of fault at base of caprock
6/2009	Completed initial CO_2 reactivity experiments for end member samples

5.Reporting Period Summary Accomplishments

In support of Task 1.0, we have participated in several telecons with members of the JIP. In May, the JIP provided a new model for the elastic properties of the overburden and underburden. Also in support of Task 1.0, LLNL hosted a coupled geomechanical and flow modeling workshop in April, 2009 in Pleasanton, California. This meeting included participants from the ISP and currently-funded second-party researchers. The goal of the meeting was to ensure continued communication across participants and encourage synergies among these different research efforts. Workshop participants included Lawrence Livermore National Laboratory (LLNL), Lawrence Berkeley National Laboratory (LBNL), BP, StatoilHydro, MDA, Pinnacle, MVE and the University of Liverpool.

In support of Task 2.0, reactive transport modeling was performed to study the potential alteration of wellbore cements. Alteration of wellbore cement by reactive, CO_2-enriched fluid presents a significant concern because net volume changes associated with mineral dissolution and precipitation reactions could expand and/or initiate fractures which could serve as conduits for CO_2 migration out of the reservoir. This reactive transport model is preliminary; the assumed set of participating mineral phases and their associated reaction rates will be updated in accordance with contemporaneous experimental results..

Also in support of Task 2.0, NUFT simulations were performed at the reservoir scale. These 3-D simulations are investigating the combined influence of heterogeneity and anisotropy upon the flow of CO_2 in the vicinity of KB-502 and KB-5. During the reporting period, a *hypothetical* vertically extending fault, conducting fluid into the lower portion of the caprock, was added. Geomechanical analysis performed under Task 3.0 identified which faults are most likely flow conduits and which are expected to act as flow barriers for inclusion into these reservoir models. NUFT simulations were performed based upon this information and the results indicate that the presence of faults in the vicinity of the KB-502 injector may be responsible for the early breakthrough of CO_2 observed at KB-5.

In support of Task 3.0, the geomechanical work proceeded on several fronts. Firstly, preliminary assessment of the stability of fractures in the overburden was performed. This is intended to provide initial predictions of the potential for fractures in the overburden to be conduits for fluid flow. This work concluded that the in situ stress state as reported will tend to induce shear on fractures in the overburden above a depth of 1600m. Secondly, the uplift of the overburden resulting from the latest NUFT reservoir models of fluid injection was predicted and compared with the InSAR data. By including conducting faults into our reservoir and overburden model we achieve better agreement with the observed net uplift at the ground surface. In short, our investigations have shown that the magnitude of uplift above Kb-502 can be achieved with fluid flow within the reservoir only. However, by including flow into a *hypothetical* fault into the lower caprock, the latest results better match the morphology of the surface deformation observed via InSAR. Our results indicated that the best fit was obtained through a combination of reservoir and fault pressurization (rather than either alone). Specifcally, the deformation due to pressurization of the fault alone results in unobserved depression and unrealistic separation between the uplift lobes. With the addition of deformation due to the reservoir, the lobes are brought closer together, and the depression due to the fault is cancelled by uplift from the reservoir.

During the reporting period, work continued in support of Task 4.0 (Integration of Reactive Transport and Geomechanical Study Results for Field-scale Interpretation). Specifically, our geomechanical analysis predicts which faults are likely to be conductive and which are expected to act as flow barriers. These results are fed into the reservoir scale simulations to predict the effect upon plume geometry and pressure response within the reservoir. In turn, the reservoir model pore pressure prediction was integrated into a geomechanical model of the overburden to provide a prediction of the associated surface uplift. The current geomechanical simulations include the hydromechanical response due to both fluid in the reservoir and conducting faults.

6.Technical Progress Report

Task 1.0 – In Salah Storage Project Data Acquisition, Interpretation, and Information Exchange

During the reporting period the JIP provided new elastic moduli for the reservoir, underburden and overburden. Additionally, we participated in several telecons with members of the JIP. In May, the JIP provided a new model for the elastic properties of the overburden and underburden. Also in support of Task 1.0, LLNL hosted a coupled geomechanical and flow modeling workshop in April, 2009. This meeting included participants from the ISP and currently-funded second-party researchers. The goal of the meeting was to ensure continued communication across participants and encourage synergies among these different research efforts. Workshop participants included Lawrence Livermore National Laboratory (LLNL), Lawrence Berkeley National Laboratory (LBNL), BP, StatoilHydro, MDA, Pinnacle, MVE and the University of Liverpool.

Task 2.0 - Reactive Transport Studies

The geochemical reactive transport simulation effort has proceeded on two fronts: (1) multiphase flow simulation of CO_2 injection into the Krechba field, and (2) reactive transport modeling was performed to study the potential alteration of wellbore cements.

Modeling CO_2 Injection

A three-dimensional multiphase flow and transport model, implemented using LLNL's NUFT simulator, has been developed for the reservoir using porosity and permeability data provided by BP that was initially used to populate BP's STARS reservoir simulator model. In our reservoir scale modeling we mainly focused on the KB-502/KB-5 area in order to understand the early CO_2 breakthrough at the KB-5 and the observed surface uplift. Based on the reservoir geometry and structured mesh in STARS model we further refined the mesh in the KB-502/KB-5 area and included the KB-502 well path into the NUFT model. The preliminary fault map at KB-502/KB-5 was also incorporated into our model. Based upon geomechanical analysis reported under Task 3.0, several faults were identified in the vicinity of KB-502 that could be fast flow paths and flow barriers. Figure 1 shows the how the current model includes these features. After consultation with others at the April workshop, we have added a *hypothetical* extension of the F12 fault above and below the reservoir by 200m. Simulations employing this new model, like that reported in the previous quarter, indicate that the fault that cuts across KB-502 (and is predicted by the geomechanics to be highly conducting) leads to early arrival of CO_2 at KB-5, consistent with observation (Figure 2). Additionally, the saturation field (top right in Figure 2) indicates that the high permeability of the fault combined with buoyancy effects allows CO_2 to migrate to the top of the fault. Under Task 3.0, we report the induced hydromechanical deformation of the overburden associated with this result and compare with the observed surface deformation from InSAR.

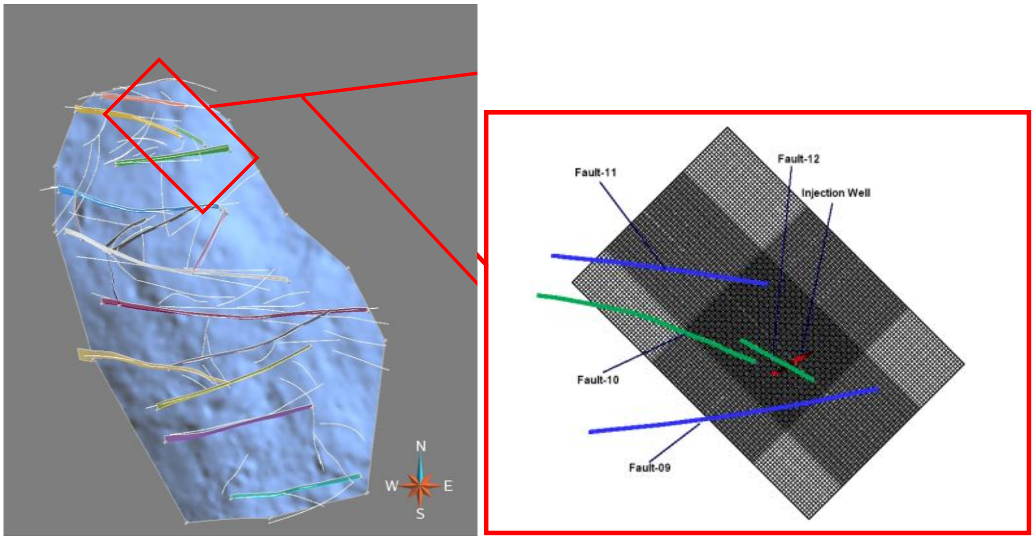

Figure 1: The NUFT model considered for the vicinity of KB-502. The green and blue lines denote permeable and impermeable faults, respectively. The permeability of permeable faults is assumed as 1 Darcy. The fault F12 was extended above and below the reservoir by 200m, to explore the effect upon deformation within the overburden**.**

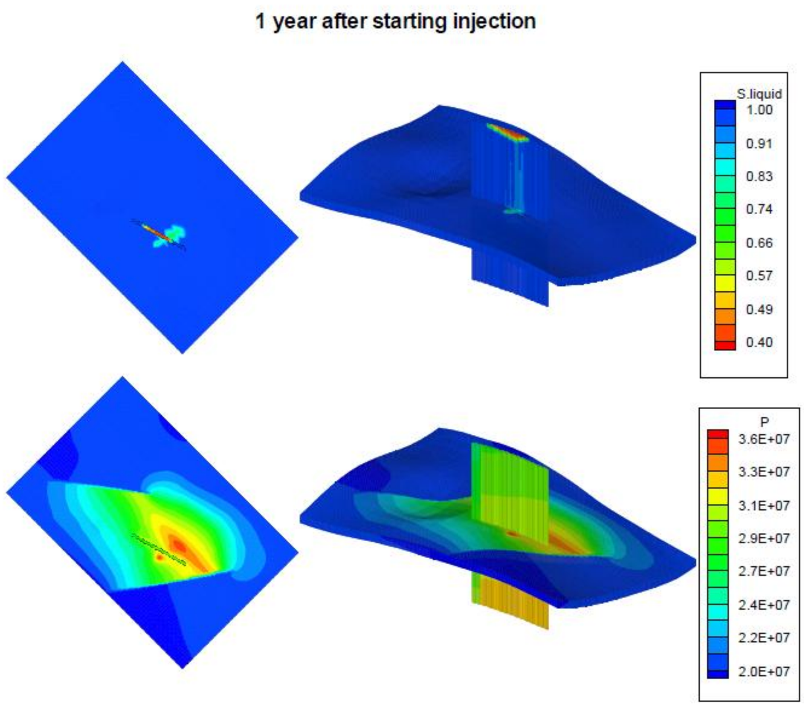

Figure 2: Result of NUFT model, including hypothetical extension of fault F12 into the overburden. The saturation field (top right) indicates that the high permeability of the fault combined with buoyancy effects allows CO_2 to migrate to the top of the fault.

Reactive Transport Modeling of Wellbore Cements

In the previous quarter, the reactive transport modeling focused on identifying key reactive mineral phases and quantifying the possible impact of mineral dissolution and precipitation reactions involving those phases on the porosity and permeability of the reservoir and the caprock.

During the current reporting period, the focus was upon predicting the reponse of wellbore cements to CO_2. Alteration of wellbore cement by reactive, CO_2-enriched fluid presents a significant concern because net volume changes associated with mineral dissolution and precipitation reactions could expand and/or initiate fractures which could serve as conduits for CO_2 migration out of the reservoir. To begin evaluating this issue for the Krechba brine composition, a one-dimensional reactive transport model comprised of a simulated section of cement in contact with formation materials was used to identify the types of mineralogical alterations that would be predicted through thermodynamic considerations and to quantify the associated net volume changes. This reactive transport model is preliminary; the assumed set of participating mineral phases and their associated reaction rates will be updated in accordance with contemporaneous experimental results.

Model Setup

Model setup is depicted on Figure 3. Plug flow is assumed to occur through a 1-cm-thick fractured zone at the interface between the formation and the cement. This zone is assumed to be characterized by a permeability of approximately 0.5 mD and is subject to a constant applied vertical pressure gradient of 0.2 bar/m. Depending on the vertical position (indicated by the y-axis), the fractured zone mineralogy is comprised of either that of the reservoir sandstone or that of the cap rock mudstone, as indicated on the figure. The initial cement mineralogy consists of a mixture of an amorphous hydrated calcium silicate solid solution (the CSH0.36 member, in this example), portlandite, and monosulfate (thermodynamic data courtesy of Bill Carey, Los Alamos National Laboratory). The model grid is discretized into 40 volume elements in the vertical direction (2-m spacing) and 11 volume elements in the horizontal direction (1.5-cm spacing).

At time $t = 0$, a CO_2-rich fluid, defined by the equilibration of a separate CO_2 fluid phase with the Krechba brine composition at T = 95C and P = 200 bars, is introduced into the model at the lower left boundary. This fluid is allowed to move through the fractured zone along the left boundary (idealized as simple plug flow) at a constant rate over a period of approximately 10 years (or 45 pore volumes, given the hydrologic constraints listed above). Transport of dissolved constituents into and out of the adjacent cement material is assumed to occur by molecular diffusion only.

Changes to solution chemistry and mineral assemblages at each location in the model were modeled using the PHREEQC geochemical speciation model, employing the one-dimensional transport capability with the stagnant cells option. All reactions were modeled assuming local thermodynamic equilibrium. For the cement interior, this assumption represents a plausible first approximation since the transport of aqueous components is diffusion-limited.

Implied volume changes, and hence changes in porosity, were tabulated in the model run but potential impacts to transport properties, such as the effective diffusion coefficient of aqueous components, were not calculated.

Results

Simulated distributions of water quality indicators – dissolved CO_2 and the associated pH impact – after 10 years are depicted on Figure 4 and Figure 5, respectively. The highest concentrations of dissolved CO_2, approximately 0.8 mol/kgw, are found within the fractured zone near the inlet. Diffusive transport of CO_2 into the cement is mitigated through reactions with cement components. Distributions of two of the cement constituents, CSH0.36 and portlandite (Figure 6 and Figure 7, respectively), indicate substantial weathering of the cement in the area corresponding to the elevated CO_2/reduced pH conditions. The principal weathering products (precipitates) consist of aragonite and amorphous silica (Figure 8 and Figure 9, respectively), with lesser quantities of brucite, siderite, goethite, gibbsite, and gypsum also appearing, as indicated on Figure 10 through Figure 14, respectively. For some mineral phases which contain components not present in the idealized cement composition in this simulation (e.g., Fe and Mg), the components are supplied through diffusive transport of brine. As a result, mineral phases such as brucite – $Mg(OH)_2$, and goethite – FeO(OH), tend to form along the boundary between the low-pH, CO_2-rich brine and the high-pH pore fluid stemming from contact with the cement. All contour plots depicting mineral phase distributions are scaled relative to 50 mol/kgw (i.e., with reference to aragonite, the most abundant mineral phase in the simulation on a molar basis).

The impact on porosity in this particular simulation is shown on Figure 15. The net result of mineral precipitation and dissolution reactions is an increase in porosity within the cement in the vicinity of the inlet boundary at the lower left. This modeled result reflects the variety of assumptions used to define this particular initial simulation in terms of mineralogy as well as transport; ongoing reactive transport modeling is intended to separately resolve the impacts of these assumptions, including:

- Cement composition, including dependence on assumed hydrated calcium silicate solid solution member as well as trace constituents that harbor components such as Mg.
- Weathering product composition, including both major and minor phases (e.g., Figure 16). Inclusion of clay minerals such as kaolinite or tobermorite in the model may be of particular significance in predicting changes in porosity.
- Reaction rates, both for dissolution as well as precipitation.
- Boundary conditions (i.e., sensitivity to flow rate along the left boundary; effect of diffusive transport of aqueous components into the formation, in addition to the cement).
- Redox buffering.

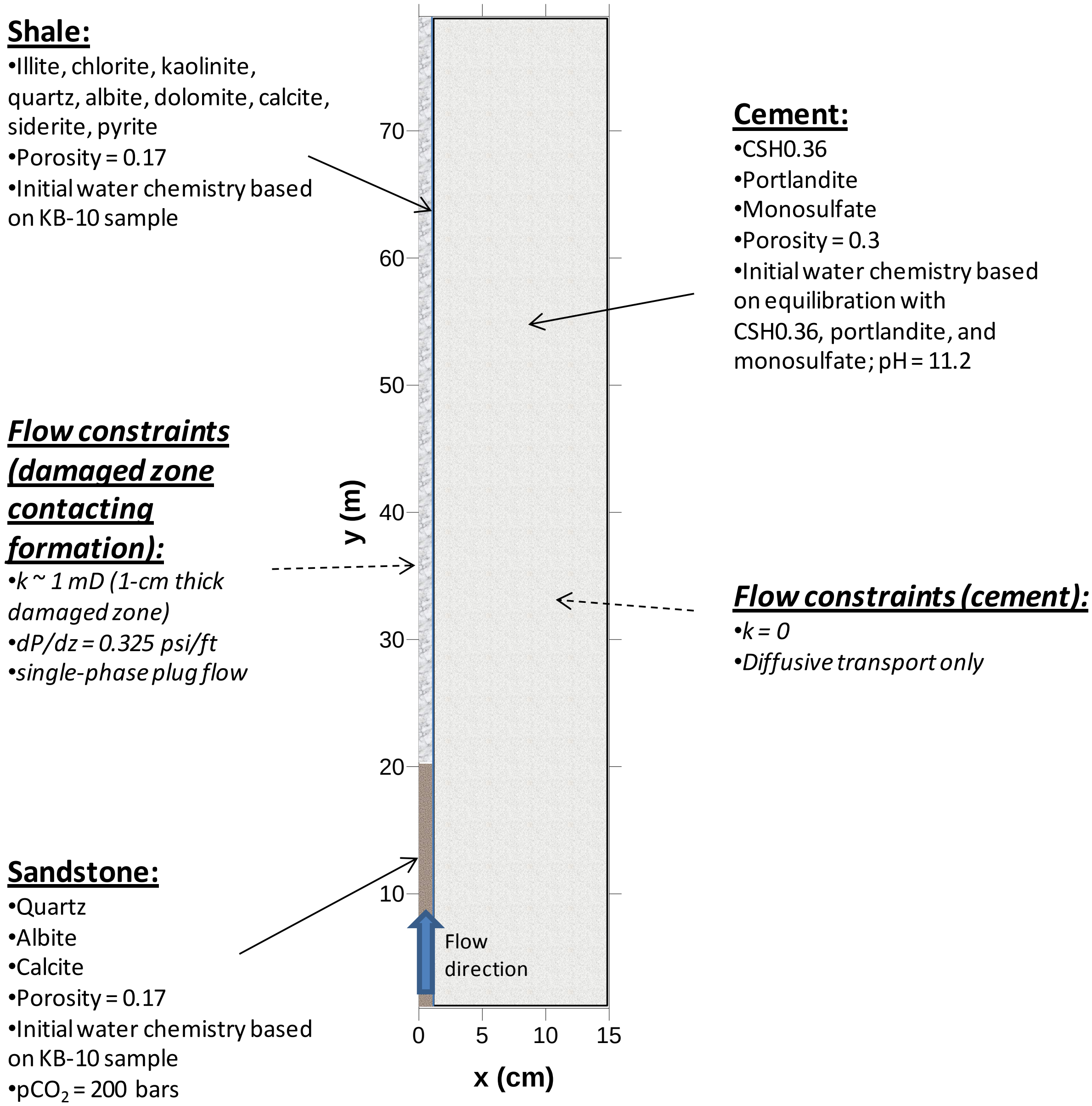

Figure 3: Cement model setup, with steady plug flow of CO_2-enriched fluid directed upward along the left boundary, in contact with formation composition along the left boundary and the (initial) cement composition on the right.

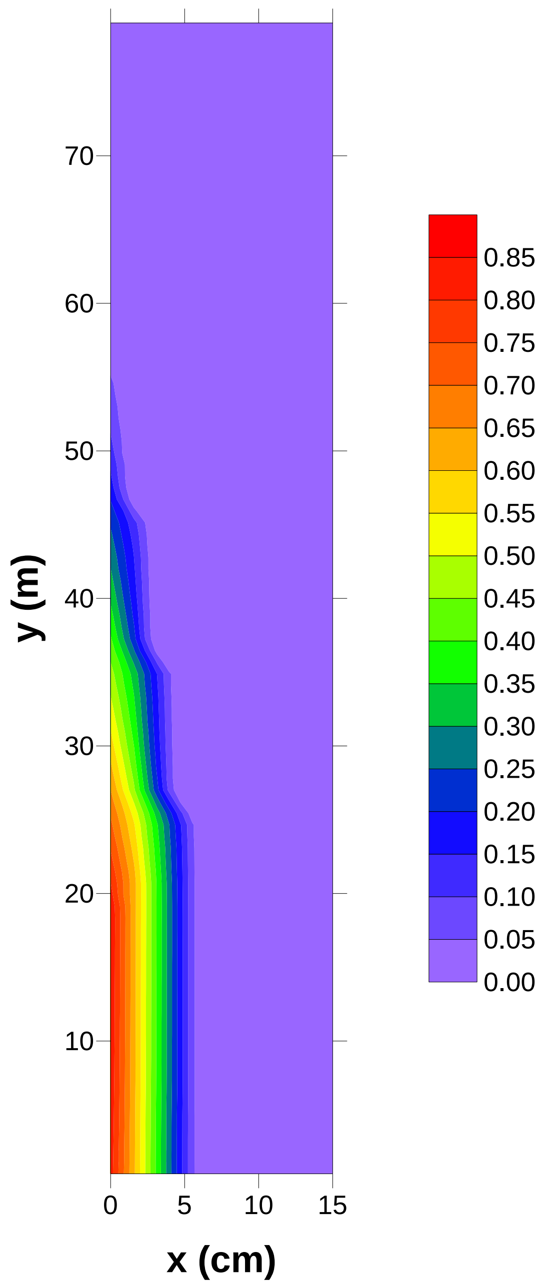

Figure 4: Simulated distribution of dissolved CO_2 (as mol/kgw) after 45 pore volumes of CO_2-enriched fluid has moved upward along the left boundary of the model domain (approximately 10 years elapsed time).

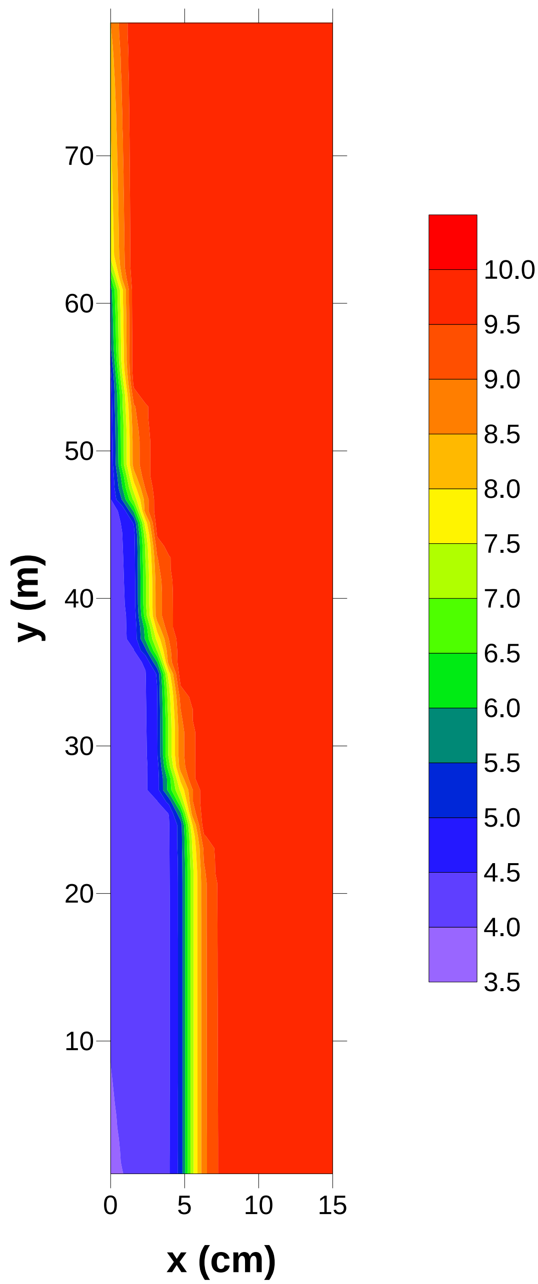

Figure 5: Simulated distribution of pH after 45 pore volumes of CO_2-enriched fluid has moved upward along the left boundary of the model domain (approximately 10 years elapsed time).

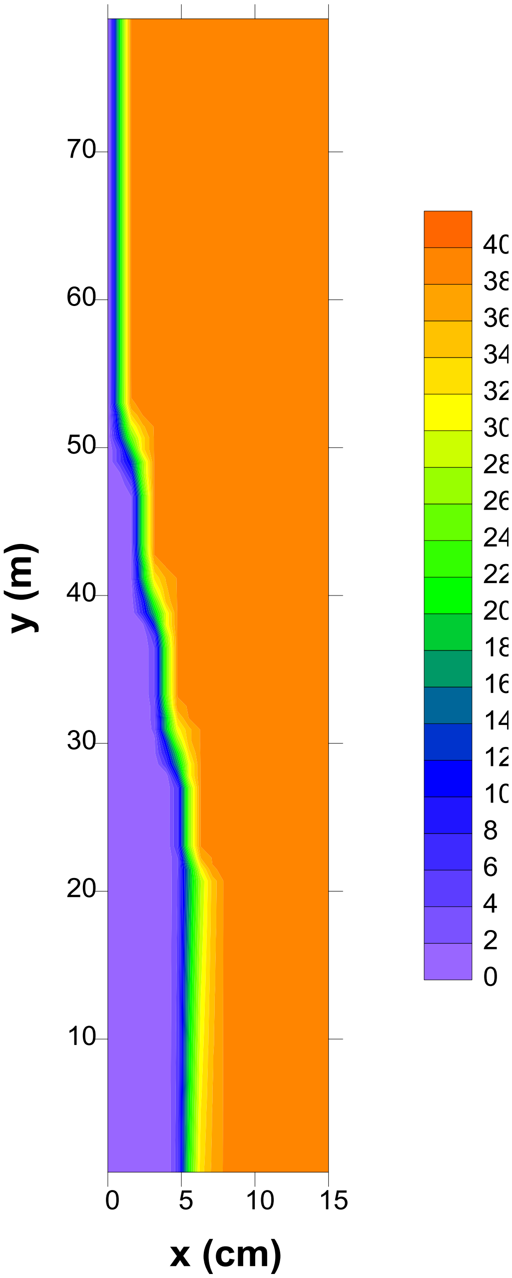

Figure 6: Simulated distribution of fresh cement component CSH0.36 (as mol/kgw) after 45 pore volumes of CO_2-enriched fluid has moved upward along the left boundary of the model domain (approximately 10 years elapsed time).

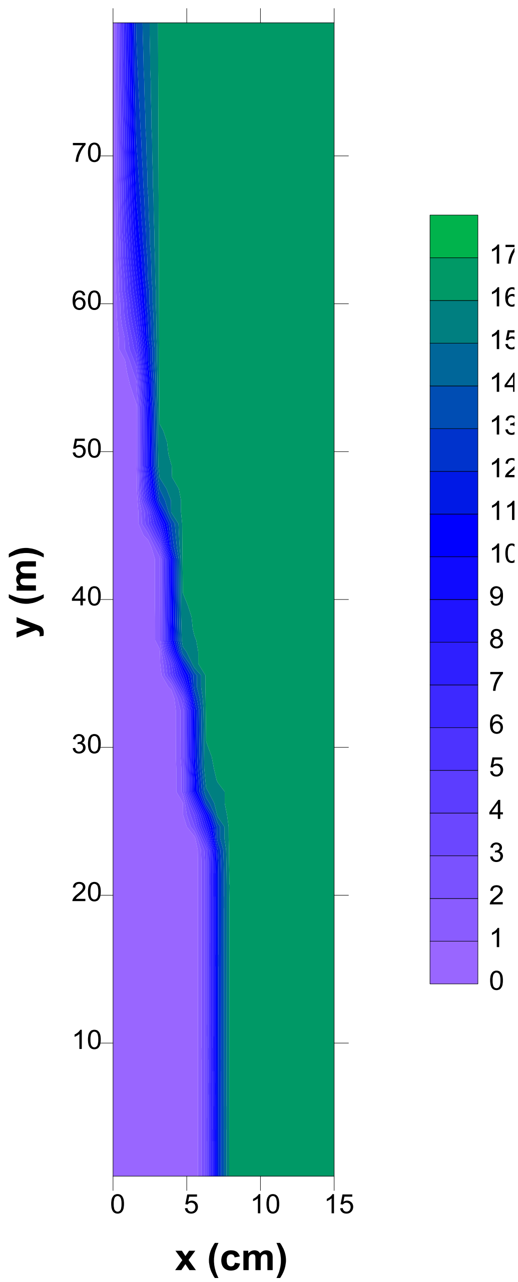

Figure 7: Simulated distribution of portlandite (as mol/kgw) after 45 pore volumes of CO_2-enriched fluid has moved upward along the left boundary of the model domain (approximately 10 years elapsed time).

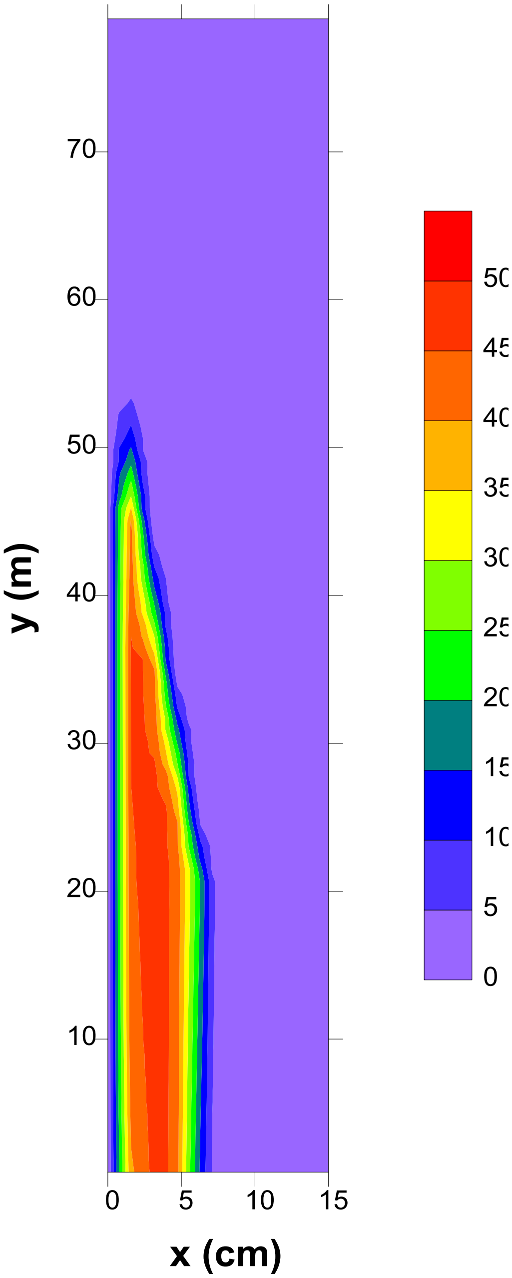

Figure 8: Simulated distribution of aragonite (as mol/kgw) after 45 pore volumes of CO_2-enriched fluid has moved upward along the left boundary of the model domain (approximately 10 years elapsed time).

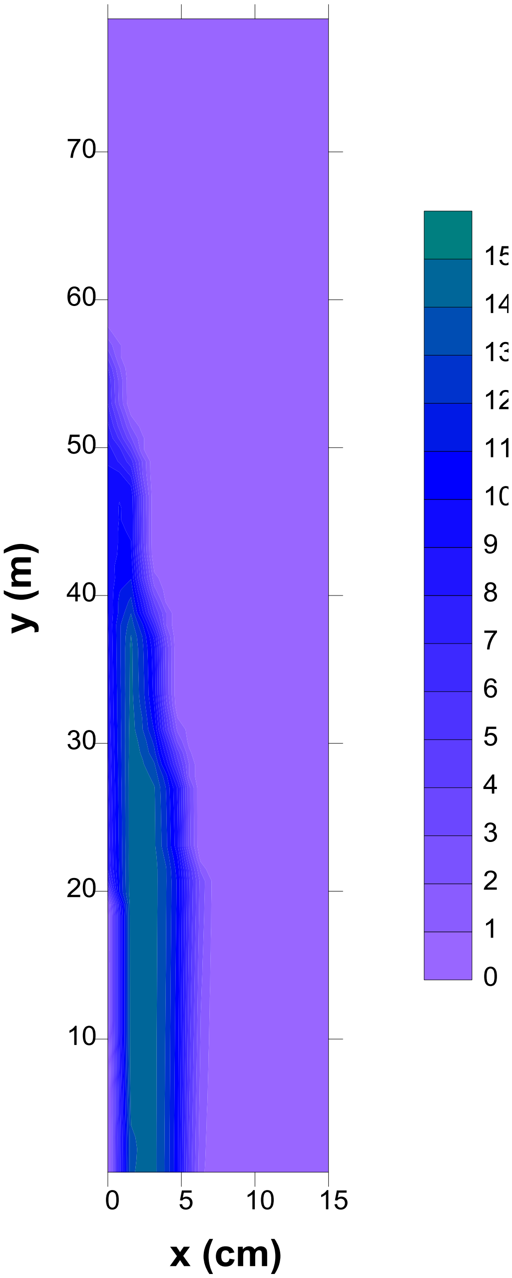

Figure 9: Simulated distribution of amorphous SiO_2 (as mol/kgw) after 45 pore volumes of CO_2-enriched fluid has moved upward along the left boundary of the model domain (approximately 10 years elapsed time).

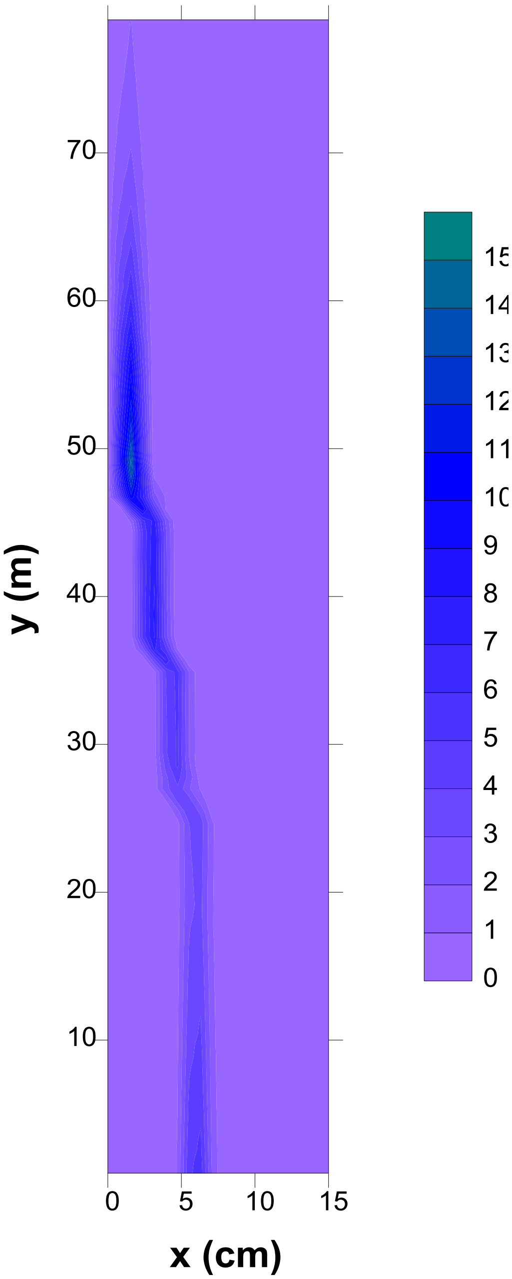

Figure 10: Simulated distribution of brucite (as mol/kgw) after 45 pore volumes of CO_2-enriched fluid has moved upward along the left boundary of the model domain (approximately 10 years elapsed time).

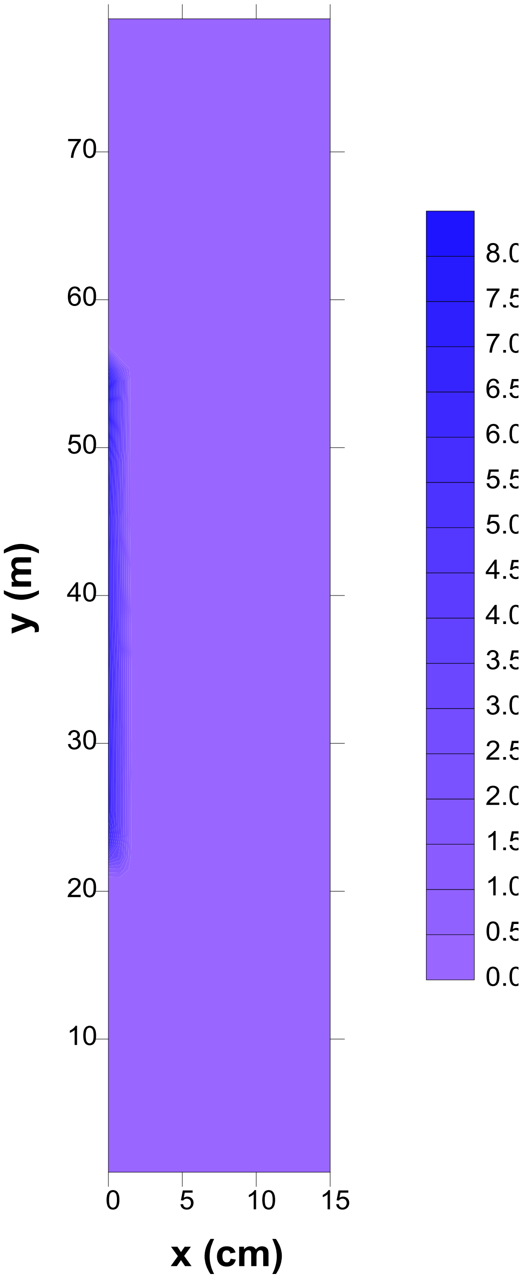

Figure 11: Simulated distribution of siderite (as mol/kgw) after 45 pore volumes of CO_2-enriched fluid has moved upward along the left boundary of the model domain (approximately 10 years elapsed time).

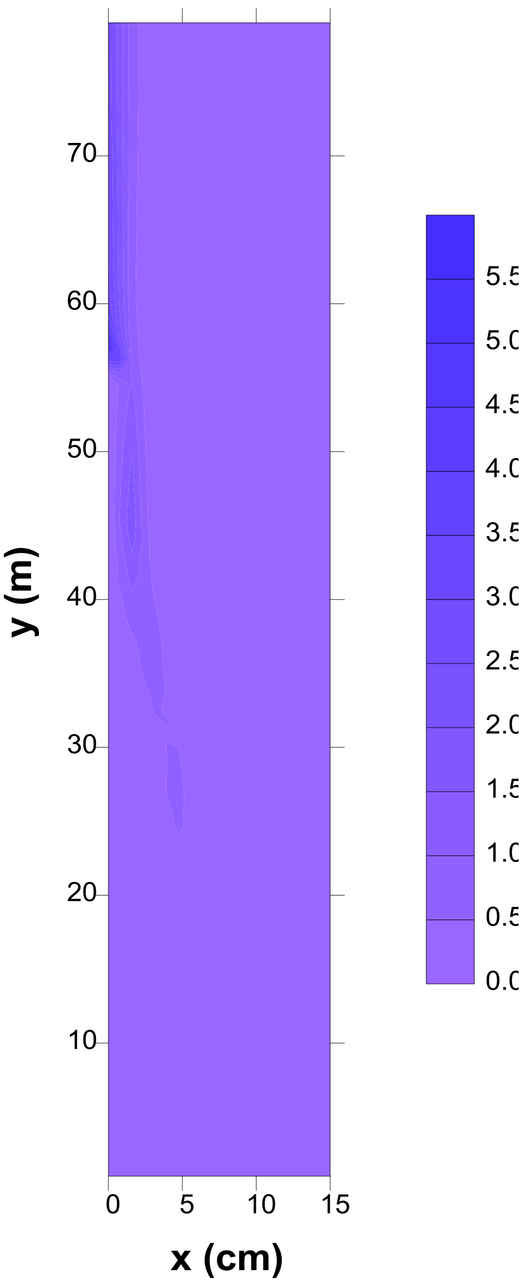

Figure 12: Simulated distribution of goethite (as mol/kgw) after 45 pore volumes of CO_2-enriched fluid has moved upward along the left boundary of the model domain (approximately 10 years elapsed time).

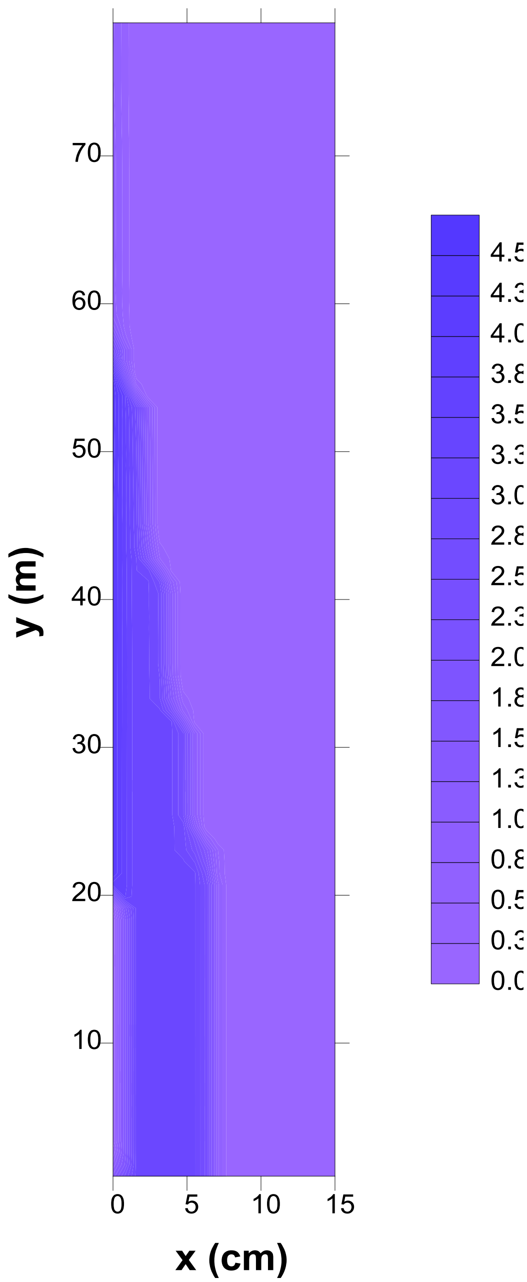

Figure 13: Simulated distribution of gibbsite (as mol/kgw) after 45 pore volumes of CO_2-enriched fluid has moved upward along the left boundary of the model domain (approximately 10 years elapsed time).

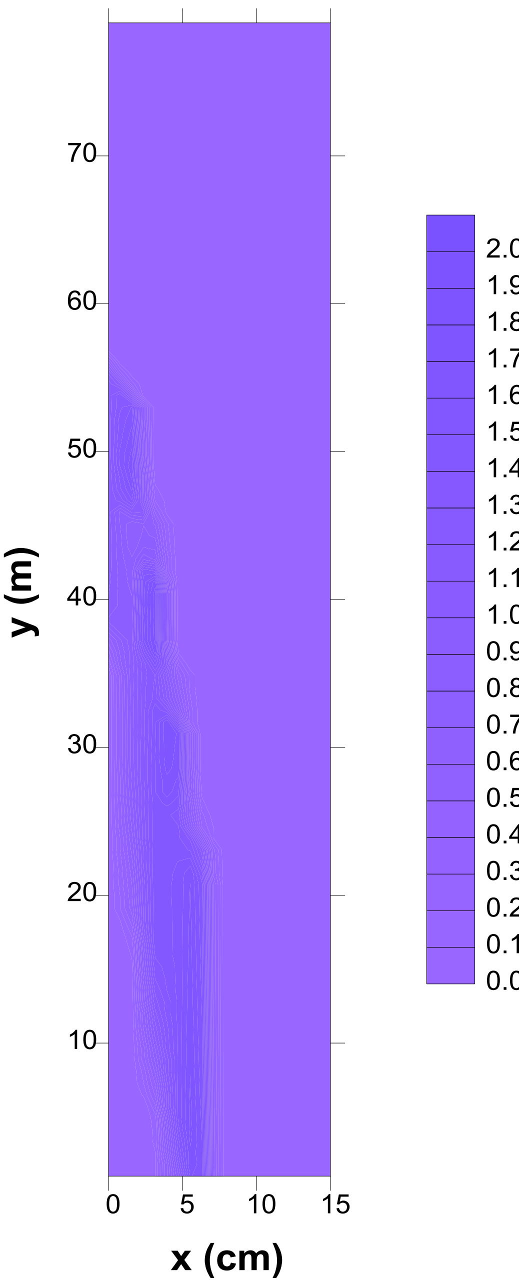

Figure 14: Simulated distribution of gypsum (as mol/kgw) after 45 pore volumes of CO_2-enriched fluid has moved upward along the left boundary of the model domain (approximately 10 years elapsed time).

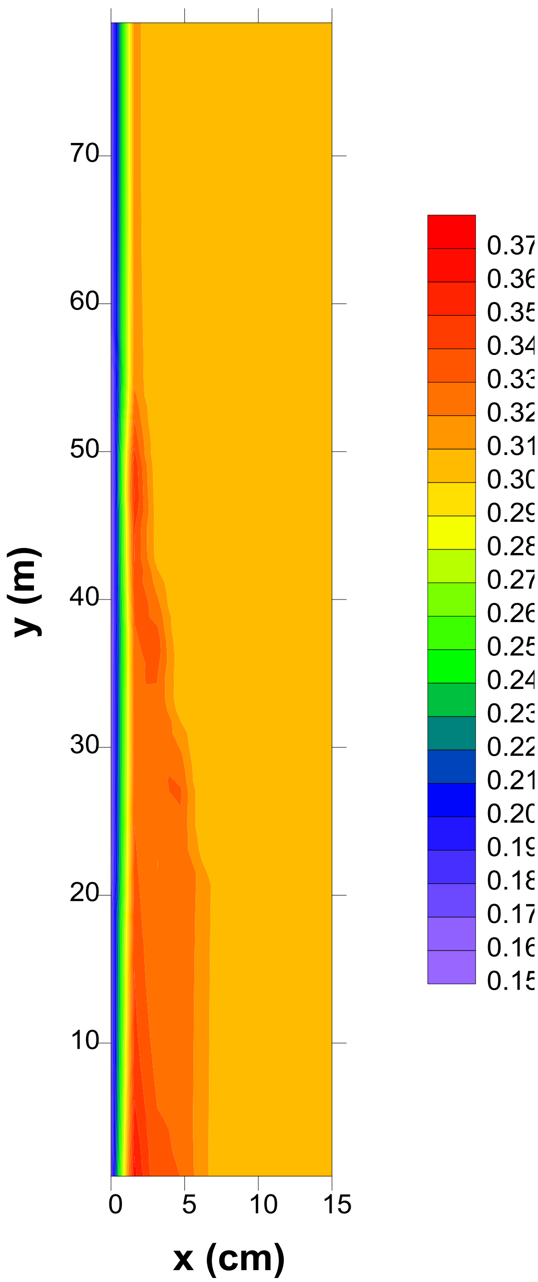

Figure 15: Simulated distribution of porosity after 45 pore volumes of CO_2-enriched fluid has moved upward along the left boundary of the model domain (approximately 10 years elapsed time).

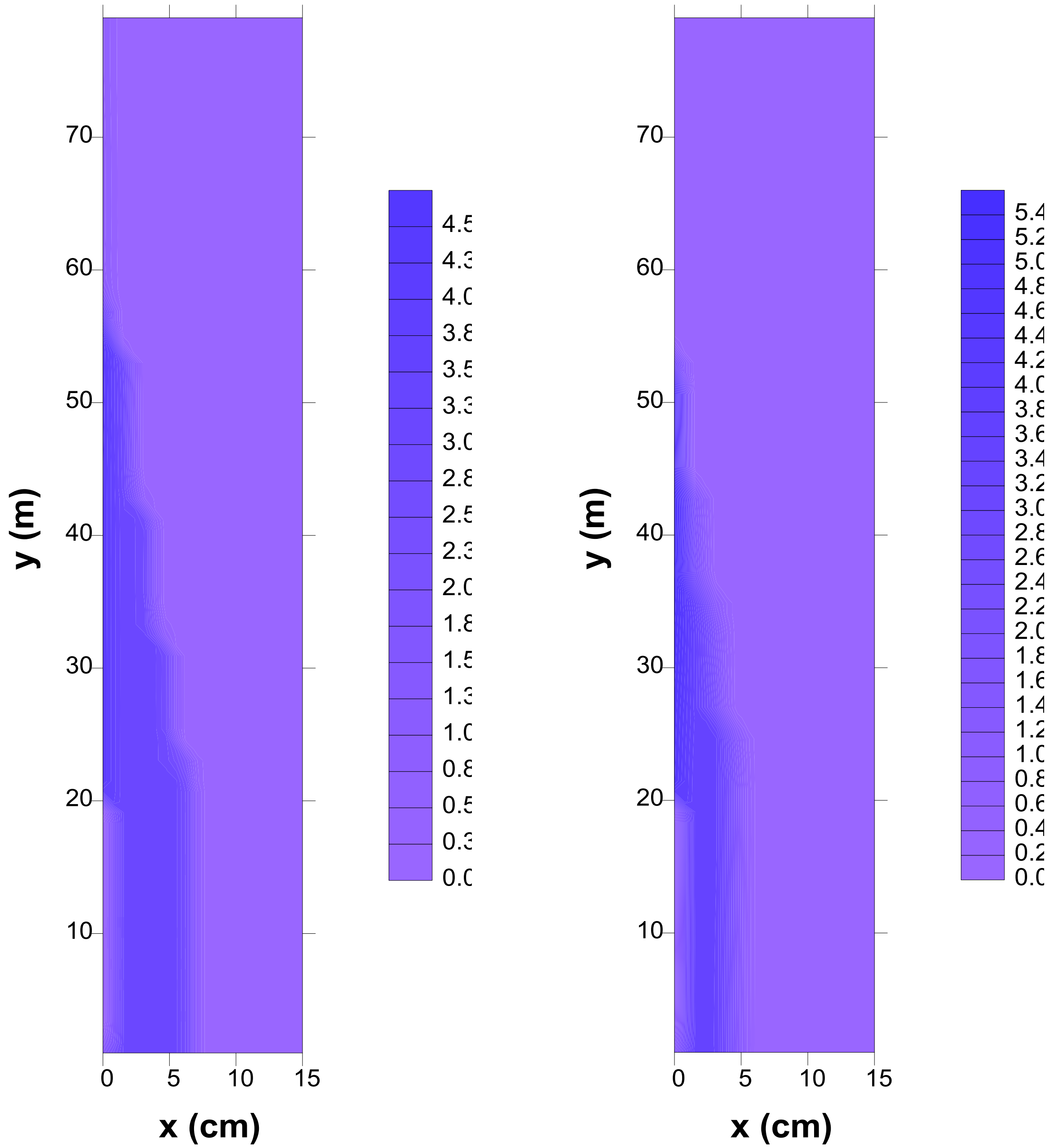

Figure 16: Simulated distributions of gibbsite (left) and dawsonite (right), under different assumptions as to the character of the aluminum-controlling phase, after 45 pore volumes of CO_2-enriched fluid has moved upward along the left boundary of the model domain (approximately 10 years elapsed time). Units are mol/kgw.

Experimental Geochemistry

The heterolithic sandstone and shale in the storage reservoir (C10.2, Figure 17) and in the overlying strata (C10.3) forms the upper section of the carbon storage reservoir at the Krechba Field, In Salah, Algeria. We have reacted the end member sandstone and shale components found in C10.2 and C10.3 with supercritical CO_2 and class G cement (plus bentonite additive) in a synthetic Krecha brine (1.8 molal NaCl, 0.55 molal $CalCl_2$, and 0.1 molal $MgCl_2$) to determine the dominant geochemical process that occur between the CO_2, cement and sandstone and shale components. This information will be used to constrain reactive transport simulations along the wellbore in the event of leakage along this pathway. In this report we present the reaction products that from on the sandstone and shale surfaces as determined by analysis with an environmental secondary electron microscope (ESEM) and energy dispersive spectroscopy (EDS). These results will be combined with solution chemistry in the next quarterly report.

Figure 17. Heterolithic tightsands (C10.2) (P. Ringrose)

The experiments consist of reacting the brine, equal weights of the class G cement (with bentonite additive) and the sandstone or the shale end members in a gold-bag autoclave at 95˚C and 100 bar. After one month of reaction, supercritical CO_2 is injected into the gold bag and reacted for an additional one month. Over the two months, several brine samples are taken and analyzed for solution chemistry. At the end of the experiment, the reaction vessel is cooled to room temperature, excess CO_2 is removed, and solid reactants are rinsed with distilled and deionized water several times to remove brine. The solids are dried at 60˚C prior to XRD and ESEM/EDS analysis.

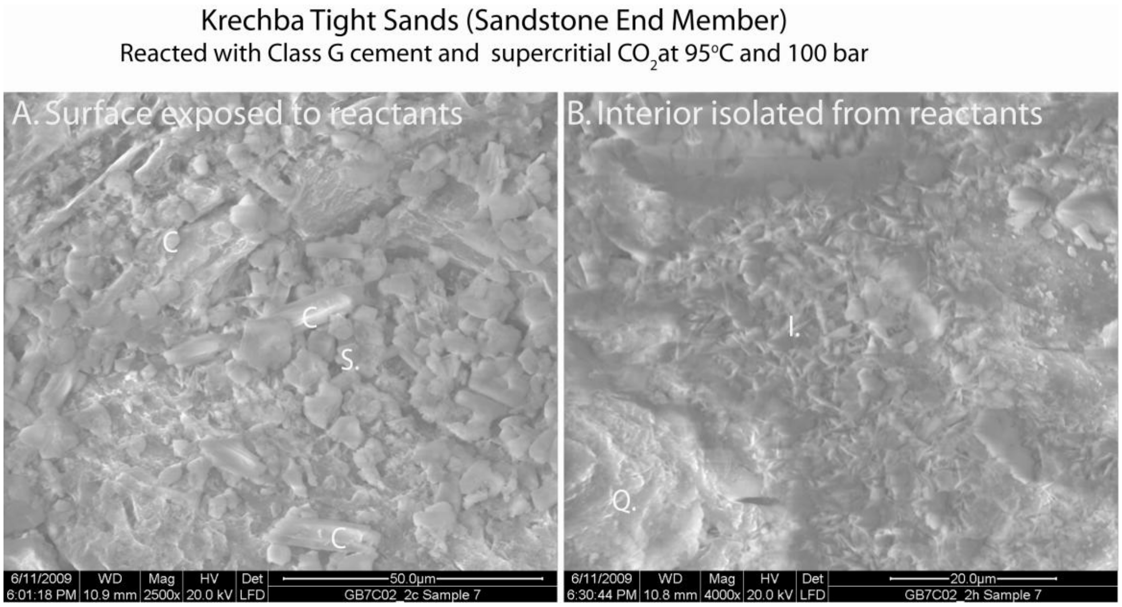

Figure 18. Electron images of a C10.2 sandstone reacted with supercritical CO_2, class G cement, and simulated reservoir brine. Image A shows a surface that was directly exposed to the reactants. Image B is a few millimeters from the surface and was not directly exposed to the surface. Letters C indicates calcium carbonate, S indicates a solid phase with calcium, silica, carbonate, chloride, and some iron, magnesium, aluminum, and chromium, Q indicates quartz, and I indicates illite (Sample 7, KB501 in Armitage 2008).

Sandstone + brine + cement + CO_2

Figure 18 shows two images of sandstone after reaction with brine, cement, and supercritical CO_2. Preliminary XRD analysis of the reacted cement suggests that the initial anhydrous calcium silicate cement phases fully reacted to amorphous silica, calcite, and aragonite, consistent with results from experiments without sandstone or shale. Sandstone provides additional dissolved silica for mineral precipitation as well as a solid surface for the accumulation of minerals precipitates in our experiments. The sandstone surface that was directly exposed to the CO_2-rich brine is covered with prismatic, well crystalline calcium carbonate, and a more amorphous looking solid made of calcium, silica, carbon, chloride, and some aluminum, iron and magnesium, sulfur, and chromium as analyzed by EDS. It is possible that the EDS beam analyzes calcium carbonate, chloride, and sulfate minerals below the surface in addition to amorphous silica on the surface. The chloride would reflect residual brine trapped between the sandstone the surface precipitates. If so, then the dominant reactions are the transformation of the cement phases to amorphous silica and calcium carbonate minerals. It is also possible that quartz at the sandstone surface dissolves to provide additional silica for the precipitation of a calcium silicate carbonate phase, such as scawtite (Ca7Si6O18CO3*2H2O), with substitution of minor components. Additional analysis, perhaps with micro-XRD or TEM would be required to robustly identify the surface precipitates. Comparison of aqueous chemistry for experiments with and without sandstone will provide additional insight on the mineralogy of the secondary precipitates.

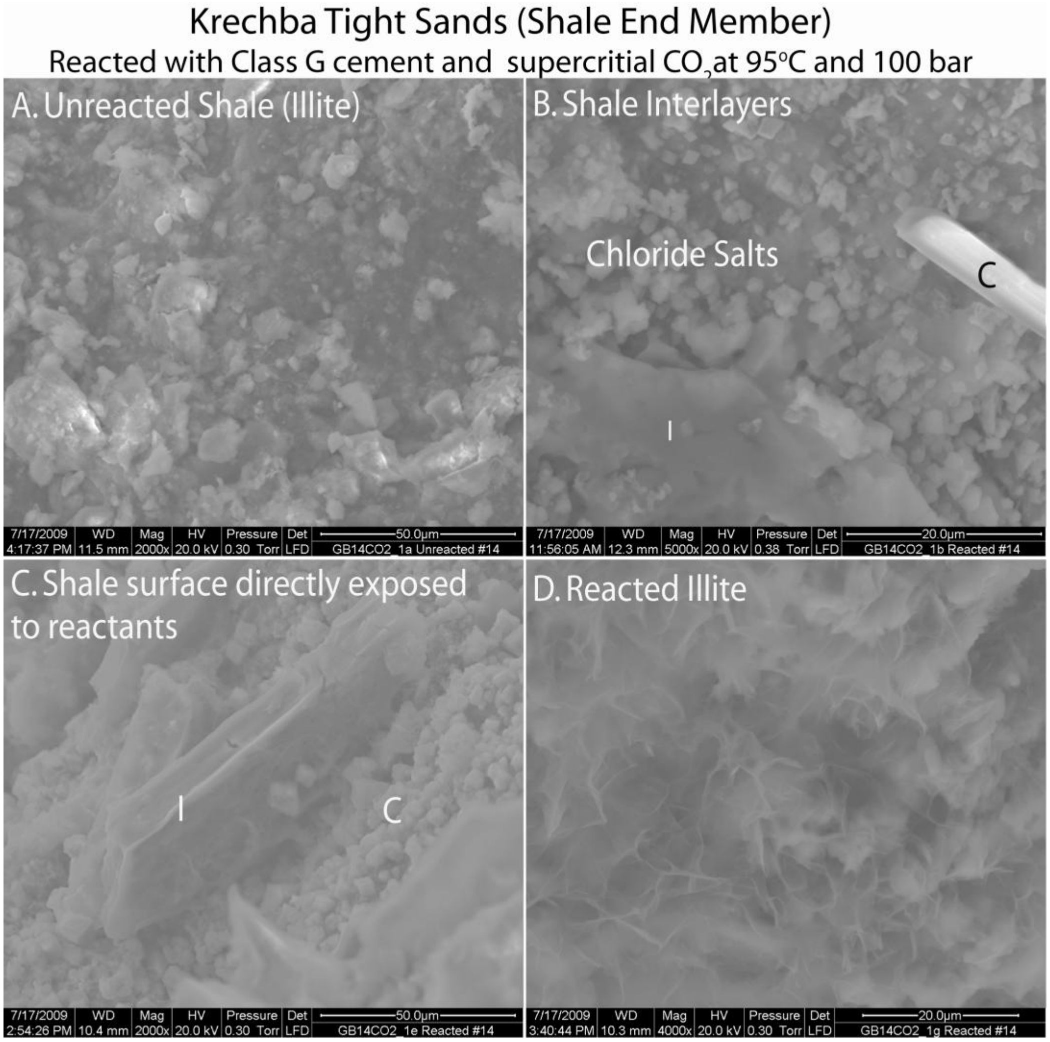

Figure 17: Figure 3. Electron images of C10.2 shale reacted with supercritical CO_2, class G cement, and simulated reservoir brine (Sample 14 in Armitage 2008). Image A shows an unreacted shale comprised mostly of illite. Images B, C, and D are from a shale surface that was directly exposed to the CO_2-rich brine. Image B shows illite with dissolution features and precipitated calcium carbonate and chloride salts that occurred between two shale layers, image C shows illite with dissolution features and significant amounts of precipitated calcite, and image D shows a reacted illite surface.

As is expected, the rock integrity is retained when sandstone is reacted with brine, cement, and CO_2, because quartz solubility and dissolution are minimal and constant from acid to slightly alkaline pH. As a result, the CO_2-rich brine does not penetrate and react with the sandstone to any great depth. Cross section analysis show no carbonate and amorphous silica reaction products even beyond the outer sandstone surface. Figure 18 shows rough quartz grain as well as a band of illite (indicated by the EDS spectra, not shown). This observation supports the notion that aqueous diffusion will limit the extent of reaction within the sandstone layers in the tight sands unit.

Shale + brine + cement + CO_2

Figure 19 shows one image of the unreacted shale and three images of the shale that was reacted with brine, cement, and supercritical CO_2. The unreacted shale shows a surface littered with illite particles that are 1 to 10 microns in length on top of larger illite surfaces.

The CO_2-rich brine reacts within the shale interlayers as well as on shale surfaces that are directly exposed to the brine. Figure 19B shows prismatic calcium carbonate crystals and cubic chloride salts formed in the shale interlayers. Illite also shows signs of reaction with the brine. The small illite grains appear to have fully dissolved, leaving behind smooth illite surfaces with dissolution pits. The salts are most likely residual brine that was not washed away at the end of the experiment. The evidence of brine in the shale interlayers suggests that permeability between shale layers must be included to appropriately model well-bore integrity between the cement and shale-rich layers within the tight sands and within the overlying cap rock.

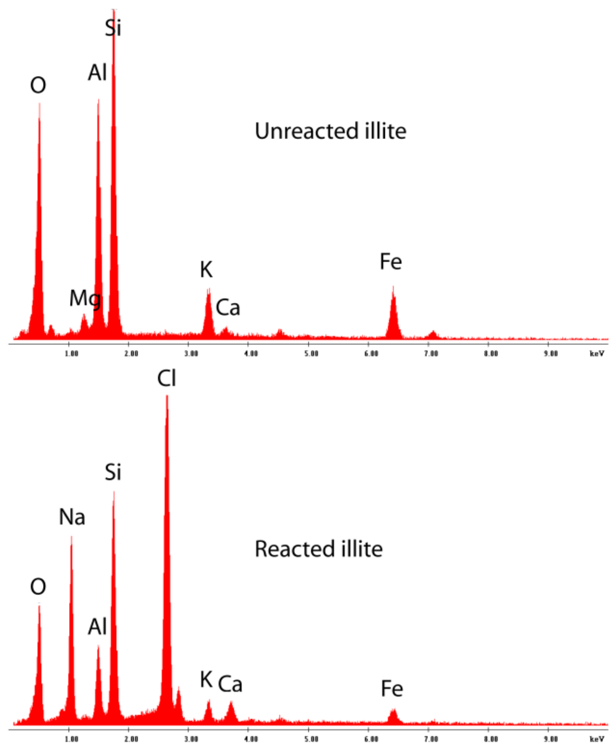

Figure 18: Figure 4. EDS spectra for unreacted shale shown in Figure 2A and reacted shale shown in Figure 2D.

Reaction of the shale is distinct from the reaction of the sandstone when directly exposed to the CO_2-rich brine and the cement. Although both surfaces show an accumulation of calcium carbonate precipitates, there was no mass precipitation of the amorphous silica phase as was observed for the sandstone (Figure 18). Instead we see dissolution etch pits as well as the formation of a fibrous precipitate at the illite surface. It is not possible to determine the composition of the fibrous precipitate with EDS analyses. EDS analysis show that expected potassium, aluminum, silica peaks for unreacted illite. But EDS spectra for reacted illite show significant amounts of chloride and sodium in addition those peaks identified for unreacted illite (Figure 20). The additional sodium, enhanced calcium and chloride may be due to salt crystals that are trapped within the altered illite but not resolved at this magnification. It may also indicate the precipitation of a distinct phase.

Task 3.0 Geomechanical Studies

In support of Task 3.0, the geomechanical work proceeded on several fronts. Firstly, preliminary assessment of the stability of fractures in the overburden was performed. This is intended to provide initial predictions of the potential for any pre-existing fractures in the overburden to act as conduits for fluid flow. Secondly, the deformation of the overburden resulting from the latest NUFT reservoir models of fluid injection was predicted and compared with the InSAR data. By including conducting faults into our reservoir and overburden model we achieve better agreement with the observed net uplift at the ground surface.

Initial Overburden Fracture Stability Assessment

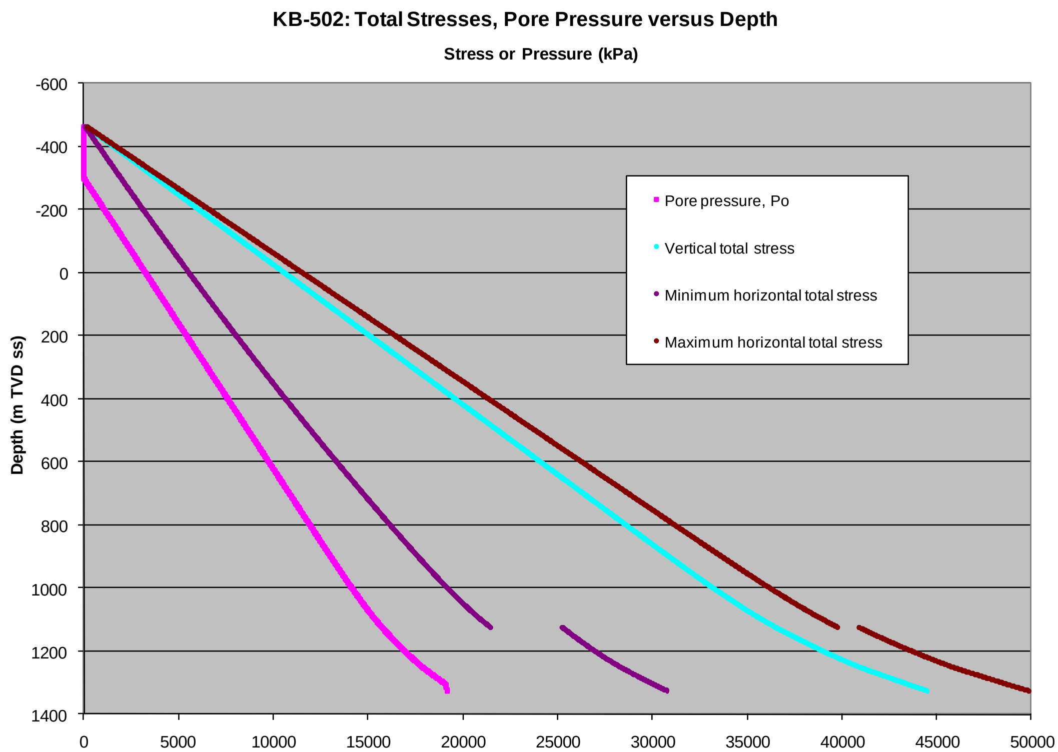

Figure 19: Variation of in situ stress and hydrostatic pressure for KB-502 as reported in Stress_Model_kb-502 model.xls and "Krechba Overburden Review.doc" (Toby Darling, April, 2006) report on the DVD provided to LLNL in June, 2008. Note the reported discontinuity at 1124 m TVDSS in the lateral stresses.

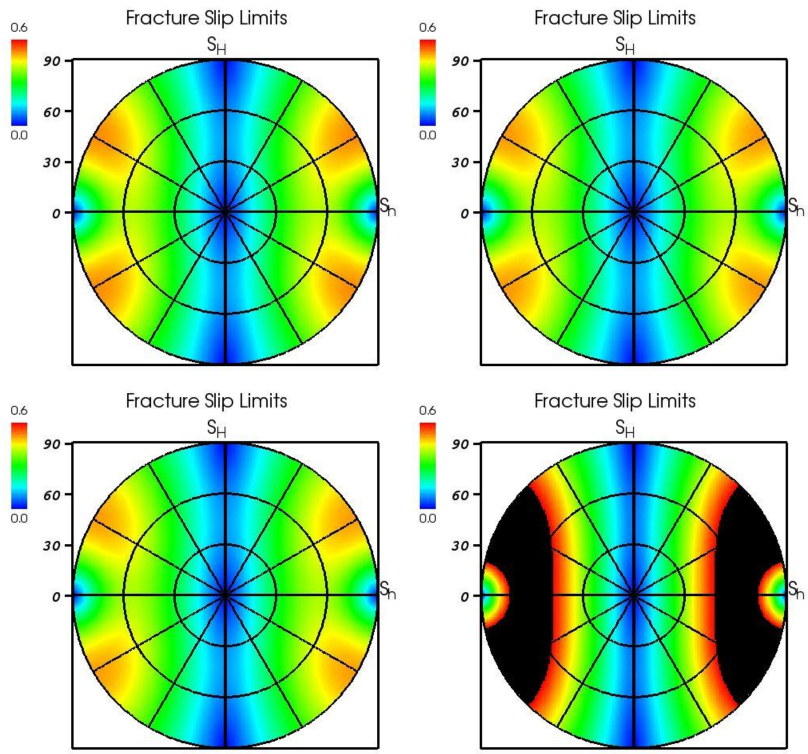

Figure 20: Calculations of fracture stability with decreasing TVDSS of 1291m, 1180m, 1124m, 1109m utilizing reported in situ stresses. Note that the discontinuity above 1124m TVDSS results in a transition to a stress state that is expected to induce shear on fractures at a range of orientations.

During the reporting period, we commenced a study of the stability of the overburden by performing analyses of the influence of pore pressure on fracture stability in the overburden covering an interval several hundred meters above the Kb-502 injector. Figure 19 shows the reported variation of in situ stress above the Kb-502 injector. The interpretation provided to us implies a strong discontinuity in the lateral stresses at approximately 1124m TVDSS. If we consider this transition with increasing elevation, the key observation is that the minimum horizontal stress undergoes a significant reduction moving from 1124m TVDSS to 1109m TVDSS, while the changes in the other stresses are less significant. The implication is that the induced shear stress at 1109m TVDSS is much greater than that at 1124m TVDSS. Consequently, it is anticipated that the reported in situ stress state at 1109m TVDSS will have a stronger propensity for inducing shear failure on pre-existing fractures, potentially leading to increased permeability of appropriately oriented fractures above 1109m TVDSS.

Figure 20 shows our prediction of propensity for shear failure in the overburden above Kb-502 for *unperturbed* hydrostatic pore pressure conditions. This analysis was performed by projecting the in situ stress state at Kb-502 onto hypothetical fracture orientations to determine what coefficient of friction is required to stabilize fractures against shear failure. The plots in Figure 20 correspond to increasing elevation above the Kb-502 injector. The color scale reflects the coefficient of friction required to maintain stability of the fractures. We make the standard assumption that the coefficient of friction cannot exceed 0.6 and black out such orientations in the plot. Consequently, the black regions of the plots correspond to fracture orientations that are expected to fail in shear and develop enhanced permeability. These results indicate that the sudden change in lateral in situ stress above 1124m TVDSS results in a transition to a stress state that is expected to induce shear failure on a range of fracture orientations. The implication is that, for the reported stress state, there is the possibility that appropriately oriented fractures in the overburden above 1124m TVDSS will be permeable to fluid flow under in situ conditions.

Figure 21 shows the coefficient of friction required for stability in the overburden above Kb-502 in the presence of a 5 MPa increase in pore pressure. These results indicate that the range of orientations activated increases with elevation above Kb-502 with a sudden increase in permeability enhancement above 1124m TVDSS due to the sudden change in lateral in situ stresses.

One implication of these results is that any fluid propagating above 1124m TVDSS, may more readily permeate any existing fractures above that depth, given the reported stress field.

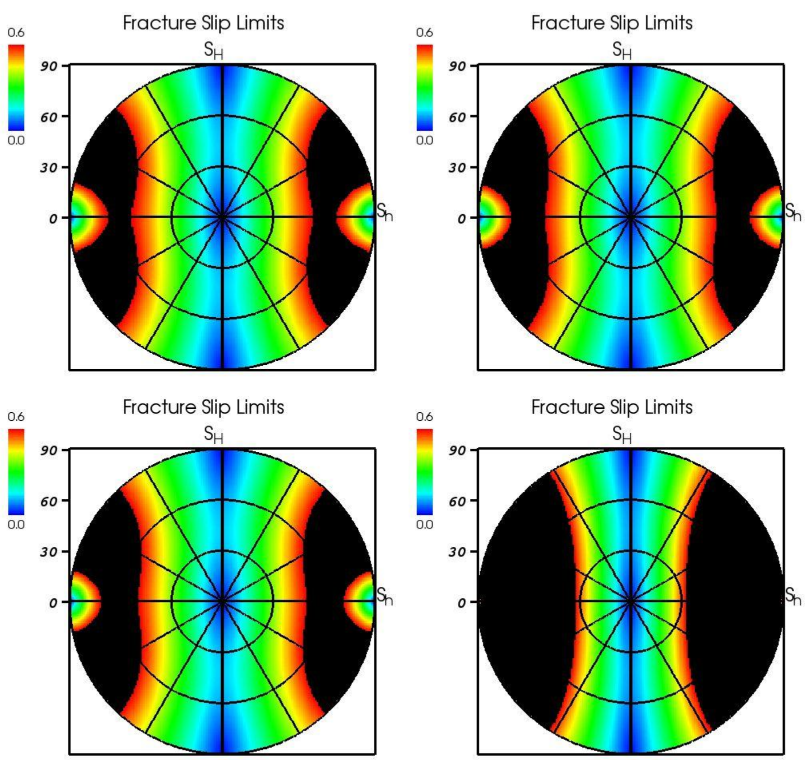

Figure 21: Calculations of fracture stability at TVDSS 1291m, 1180m, 1124m, 1109m in response to an injection pressure of 5 MPa. At all depths considered, shear failure of fractures of some orientations are predicted. Note that the discontinuity above 1124m TVDSS results in a transition to a stress state that is expected to induce more extensive shear on fractures at a range of orientations.

Prediction of Uplift due to Injection

We have performed analyses of the influence of pore pressure predictions from the NUFT analysis (Task 2.0) upon deformation of the overburden for the purpose of verifying our simulations against InSAR data. The reservoir scale simulations performed with NUFT in support of Task 2.0 were post-processed with a fast running overburden modeling tool. As documented in the discussion of Task 2.0, we investigated the influence of a *hypothetical* extension of fault F12, 200m into the lower portion of the overburden. The geomechanical calculation treated the mode of volume change within the reservoir and faults using different hydromechanical treatments. Specifically, the volume change due to hydromechanical effects within the reservoir is assumed to result in local isotropic expansion. Within the fault, because of the local geometry of the pressurized pore space, the hydromechanical effect is assumed to be that of mode I opening locally. This distinction in geomechanical treatment is important, because it results in qualitatively different effects at the surface. Specifically, the characteristic two-lobed uplift structure associated with a vertical, pressurized fault is a consequence of mode I opening displacement locally at the fault.

The mechanical properties of the hypothetical fault are at this point unknown, so we considered a range of specific normal stiffnesses: 1 GP/m, 0.1 GPa/m and 0.01 GPa/m (Figure 22 through Figure 24, respectively). These values span the expected range from a rather stiff fault to a very compliant fault. Each figure shows separately the predicted uplift associated with the fault (top left), the reservoir (top right), the combination (bottom left) and the corresponding InSAR data (bottom right). As expected, the more compliant (lower value) of specific normal stiffness, the larger the magnitude of displacements associated with the fault.

The choice of specific normal stiffness of 0.1 GPa/m for the fault appears to provide the best fit to InSAR observations (see Figure 23). These results indicate that the details of the surface uplift are captured by neither the fault induced or reservoir induced displacement alone. The surface deformation due to the reservoir alone (top right in Figure 23) lacks the morphology observed in the InSAR data, although the magnitude is reasonably correct. Additionally, these results indicate that the uplift lobes associated with the fault alone (top left in Figure 23) exhibit greater separation than those in the data. Additionally, the pressurization of the fault in isolation leads to a depression which is not observed in the data. Combining the influence of the fault with that of the reservoir has two effects:

1. The peaks of the lobes are brought closer together, to be more consistent with the data
2. The depression is cancelled by uplift due to the reservoir pressurization.

Consequently, it is only when the hydromechanical effect of the hypothetical vertical extension of F12 is included that the surface deformation adopts the shape observed via satellite.

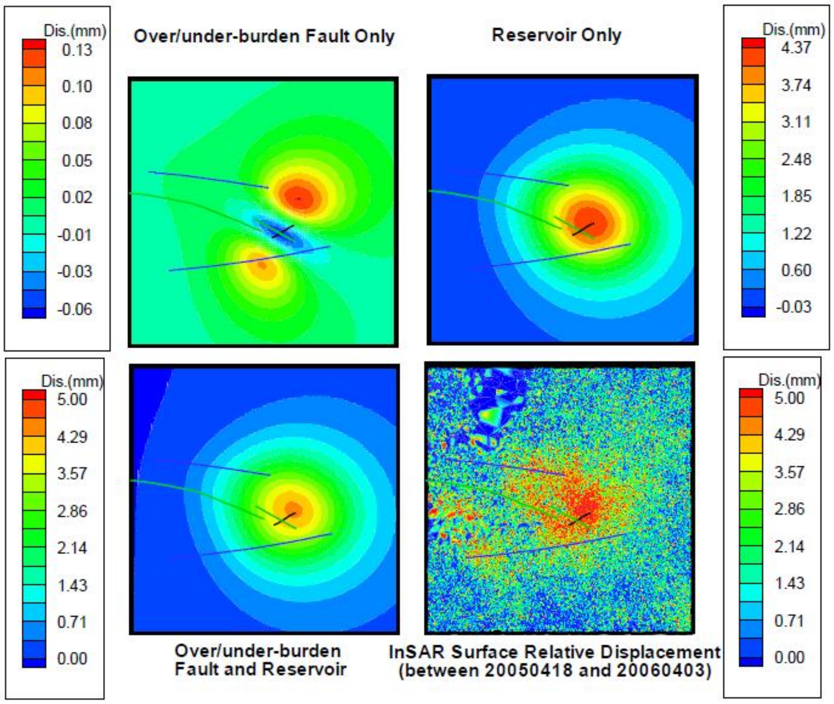

Figure 22: Comparison of predicted uplift with InSAR Data at 1 year, assuming a normal stiffness of 1 GPa/m on the fault.

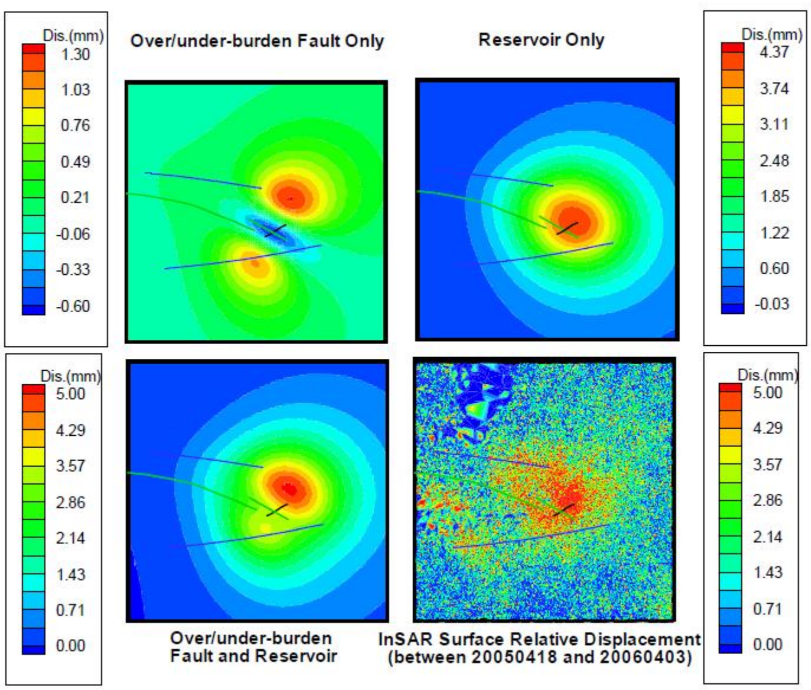

Figure 23: Comparison of predicted uplift with InSAR Data at 1 year, assuming a normal stiffness of 0.1 GPa/m on the fault.

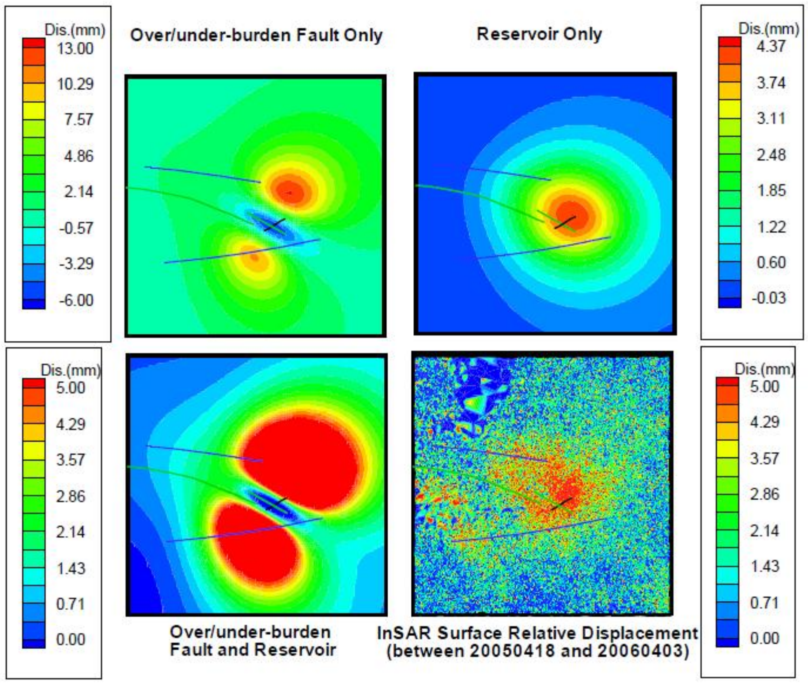

Figure 24: Comparison of predicted uplift with InSAR Data at 1 year, assuming a normal stiffness of 0.01 GPa/m on the fault.

These fast-running overburden simulations presumed a homogenous elastic overburden model. We have also commenced hydromechanical studies of this system using the LDEC code to confirm results obtained with the fast-running mechanical code. The LDEC study has the advantage of being able to accommodate arbitrary inhomogeneities within the overburden. Once an improved overburden model based upon interpretation of newly acquired 3-D seismic data by the JIP is completed, a detailed LDEC model for the overburden can be developed to determine the effect of overburden heterogeneity upon surface uplift. Additionally, we will extend the fast running model to consider layered overburden, based upon the existing overburden model provided by the JIP.

Task 4.0 Integration of Reactive Transport and Geomechanical Study Results for Field-scale Interpretation

During the reporting period, preliminary work was also performed in support of Task 4.0. Specifically, geomechanical analysis was used to predict which faults are likely to be conductive and which are expected to act as flow barriers. These results were fed into the reservoir scale simulations to predict the effect upon plume geometry and pressure response within the reservoir. In turn (as reported for Task 3.0), the reservoir model pore pressure prediction was integrated into a geomechanical model of the overburden to provide a prediction of the associated surface uplift.

Acknowledgements

This research was supported with cofounding and data provided by the In Salah Project JIP (a consortium of BP, StatoilHydro and Sonatrach).

REFERENCES:

Chiaramonte, L., M.D. Zoback, S.J. Friedmann, and V. Stamp, CO2 Sequestration, Fault Stability and Seal Integrity at Teapot Dome, Wyoming, NETL 5th Annual Conference on Carbon Sequestration, Alexandria, VA, Exchange Monitor Publications, 2006.

Detwiler, R.L., J.P. Morris and S.M. Ezzedine, Coupling micromechanics and fluid flow through discrete fracture networks: Quantifying effective permeability under variable stress conditions, Eos Transactions AGU, 86(46), Fall Meeting Supplement, Abstract H13D-1433,2006.

Duguid, A., Radonjic, M., and Scherer, G., 2005, Degradation of well cements exposed to carbonated brine: Fourth National Conf. Carbon Sequestration, Alexandria, VA, May 2-5, 005.

Johnson, J.W., Knauss, K.G, Friedmann, S.J., and Stevens, S.H., 2005b, Enhanced isolation performance of geologic CO2 storage sites through mineral trapping: Experimental and field confirmation of model predictions: Fourth National Conf. Carbon Sequestration, Alexandria, VA, May 2-5, 2005.

Johnson, J.W., Knauss, K.G., Glassley, W.E., DeLoach, L.D., and Tompson, A.F.B., 1998, Reactive transport modeling of plug-flow reactor experiments: quartz and tuff dissolution at 240oC: J. Hydrol., v. 209, p. 81-111.

Johnson, J.W., J. J. Nitao and J. P. Morris, Modeling the Long-Term Isolation Performance of Natural and Engineered Geologic CO2 Storage Sites, GHGT-7, Vancouver, BC, September 5-9, 2004.

Johnson, J.W., Nitao, J.J., and Knauss, K.G., 2004a, Reactive transport modeling of CO2 storage in saline aquifers to elucidate fundamental processes, trapping mechanisms, and sequestration partitioning: in Geol. Soc. London Spec. Pub. 233 Geologic Storage of Carbon Dioxide, Baines, S.J., and Worden, R.H., eds., p. 107-128.

Johnson, J.W., Nitao, J.J., and Morris, J.P., 2005a, Reactive transport modeling of cap rock integrity during natural and engineered CO2 storage: in Carbon Dioxide Capture for Storage in Deep Geologic Formations: Vol. 2, Thomas, D.C., and Benson, S.M., eds., p. 787-813.

Johnson, J.W., Nitao, J.J., Morris, J.P., 2004, “Reactive Transport Modeling of Cap Rock Integrity During Natural and Engineered CO_2 Storage,” in *Carbon Dioxide Capture for Storage in Deep Geologic Formations* (Elsevier: ISBN0080445705)

Kharaka Y. K., Cole D. R., Hovorka S. D., Gunter W. D., Knauss K. G., and Freifeld B. M. (2006) Gas-water-rock interactions in Frio Formation following CO2 injection: Implications for the storage of greenhouse gases in sedimentary basins. Geology 34(7), 577-580.

Knauss, K.G., Johnson, J.W., and Kharaka, Y.K., 2005, Preliminary reactive transport modeling and laboratory experiments conducted in support of the Frio pilot test: Fourth National Conf. Carbon Sequestration, Alexandria, VA, May 2-5, 2005. 10

Morris, J.P., M. B. Rubin, S. C. Blair, L. A. Glenn and F. E. Heuze, Simulations of Underground Structures Subjected to Dynamic Loading using the Distinct Element Method, Engineering Computations, Vol. 21 (2/3/4), 384-408, 2003.

Morris, J.P., Johnson, S., Friedmann, S.J., 2008, "Geomechanical Simulations of Caprock Integrity using the Livermore Distinct Element Method," 7th Annual Conference on Carbon Capture & Sequestration, Pittsburgh, Pennsylvania.

Parkhurst, D.L. and Appelo, C.A.J., 1999. User's guide to PHREEQC (version 2)--A computer program for speciation, batch-reaction, one-dimensional transport, and inverse geochemical calculations: U.S. Geological Survey Water-Resources Investigations Report 99-4259, 312 p.

Parkhurst, D.L. and Appelo, C.A.J., 1999, User's guide to PHREEQC (version 2)--A computer program for speciation, batch-reaction, one-dimensional transport, and inverse geochemical calculations: U.S. Geological Survey Water-Resources Investigations Report 99-4259, 312 p.

Parkhurst, D.L., Kipp, K.L., Engesgaard, Peter, and Charlton, S.R., 2004, PHAST--A program for simulating ground-water flow, solute transport, and multicomponent geochemical reactions: U.S. Geological Survey Techniques and Methods 6-A8, 154 p.

Petersson, N.A., A. Rodgers, M. Duchaineau, S. Nilsson, B. Sjogreen and K. McCandless, Large scale seismic modeling and visualization of the 1906 San Francisco earthquake, Seismological Society of America Annual meeting, San Francisco, April 18-22, 2006.

Riddiford, F., Akretche, S., and Tourqui, A., 2003, Storage and sequestration of CO2 in the In Salah Gas Project: 22nd World Gas Conference, Tokyo, 7p.

Riddiford, F., Wright, I., Bishop, C., Espie, T., and Tourqui, A., 2004, Monitoring geological storage: The In Salah gas CO2 storage project: GHGT-7, Vancouver, 6 p.

Wiprut D.J. and M.D. Zoback, Fault reactivation, leakage potential, and hydrocarbon column heights in the northern North Sea, Hydrocarbon Seal Quantification (NPF Special Publication) 11, 203-219, 2002.

7.Assessment of Current Status

The project continues to be on time and budget. With rock samples from Krechba being made available in the previous quarter, initial experimental work investigating CO_2 reactivity of Krechba rock was completed.

New overburden models, fault maps and microseimic data are expected in the next quarter due to recent data acquisitions made by the JIP in the current quarter.

8.Plans for the Next Quarter

The experimental program will continue to focus upon studying the reactivity of rock and cements from the Krechba field. The geomechanical studies will continue to investigate the mechanical response of the overburden and upper portion of the storage system including progressively more detailed heterogeneity. More detailed reactive transport and geomechanical studies will be enabled as the new porosity/permeability cubes are made available by the JIP from the newly acquired seismic data. Geomechanical studies into predicting the surface expression of the injected fluid will continue. New high quality InSAR data will be obtained for constraining our models in Q4. It expected that microseimic data from Krechba will be available in the next quarter and the data obtained will be transmitted to LLNL under existing data sharing agreements.

9.Attachments

Presentation at CCS 2009, Pittsburgh, May, 2009
Paper published in the proceedings of ARMA, Asheville, June, 2009
Article submitted to GEOSTRATA.

Eighth Annual Conference on Carbon Capture & Sequestration

Overview of Major CCS Projects Outside USA (2)

The Role of Injection-Induced Mechanical Deformation and Geochemical Alteration at the In Salah CO2 Storage Project

Joseph P. Morris, Walt McNab and Yue Hao

Lawrence Livermore National Laboratory

May 4 -7, 2009 • Sheraton Station Square • Pittsburgh, Pennsylvania

Eighth Annual Conference on Carbon Capture & Sequestration

LLNL-PRES-412648

Predicting fate of CO_2 requires understanding of coupled processes

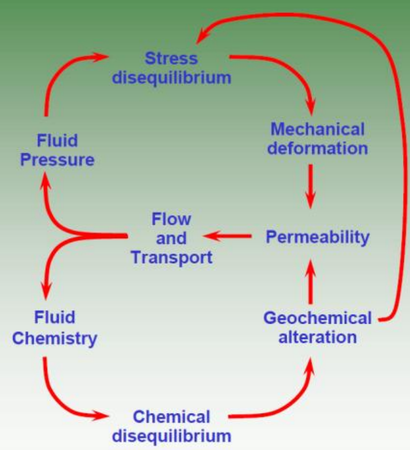

- Multiple processes are either directly or indirectly coupled
  - Relative significance of these couplings is both *site and injection scenario specific*
- Coupling is potentially exaggerated by fracture networks, e.g.:
  - Small changes in aperture → Large change in permeability
  - Creation of new fractures → new flow paths
  - Healing of fractures through precipitation → Potential for drastic reduction in permeability

Eighth Annual Conference on Carbon Capture & Sequestration

LLNL-PRES-412648

We have studied the stability of combinations of fracture networks and faults

- Fault network for the storage system
  - No faults observed in the caprock/overburden
  - Fault map courtesy of the In Salah Gas JIP

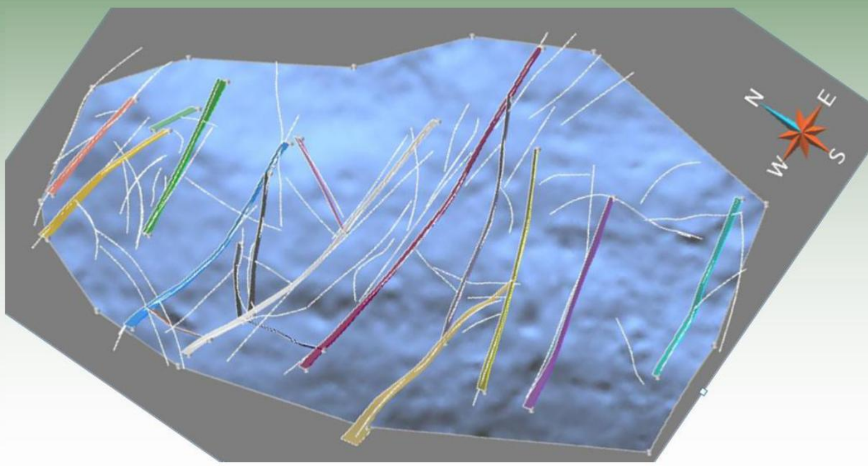

Eighth Annual Conference on Carbon Capture & Sequestration

LLNL-PRES-412648

Critical stress analysis: Evaluate change in pore pressure that induces failure

- Fast, provides overview of potential effects of fluid injection
- Estimate of change in pore-pressure that will result in shear failure of faults
- Does not provide insight into mechanical interactions once deformation occurs
- Identifies which faults are likely flow conduits or barriers

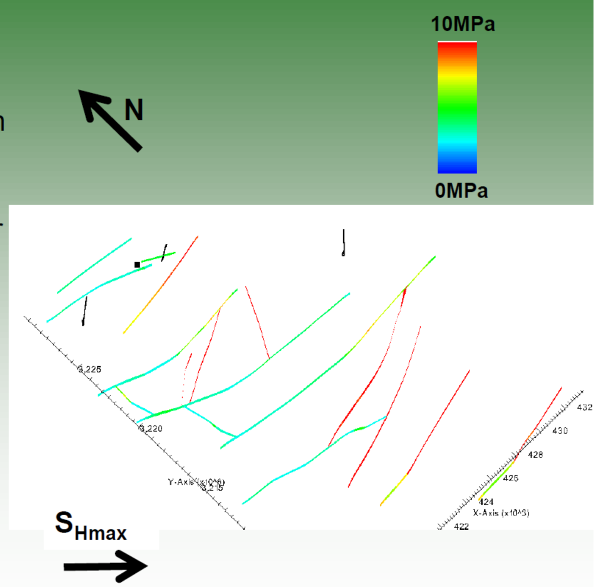

Eighth Annual Conference on Carbon Capture & Sequestration

LLNL-PRES-412648

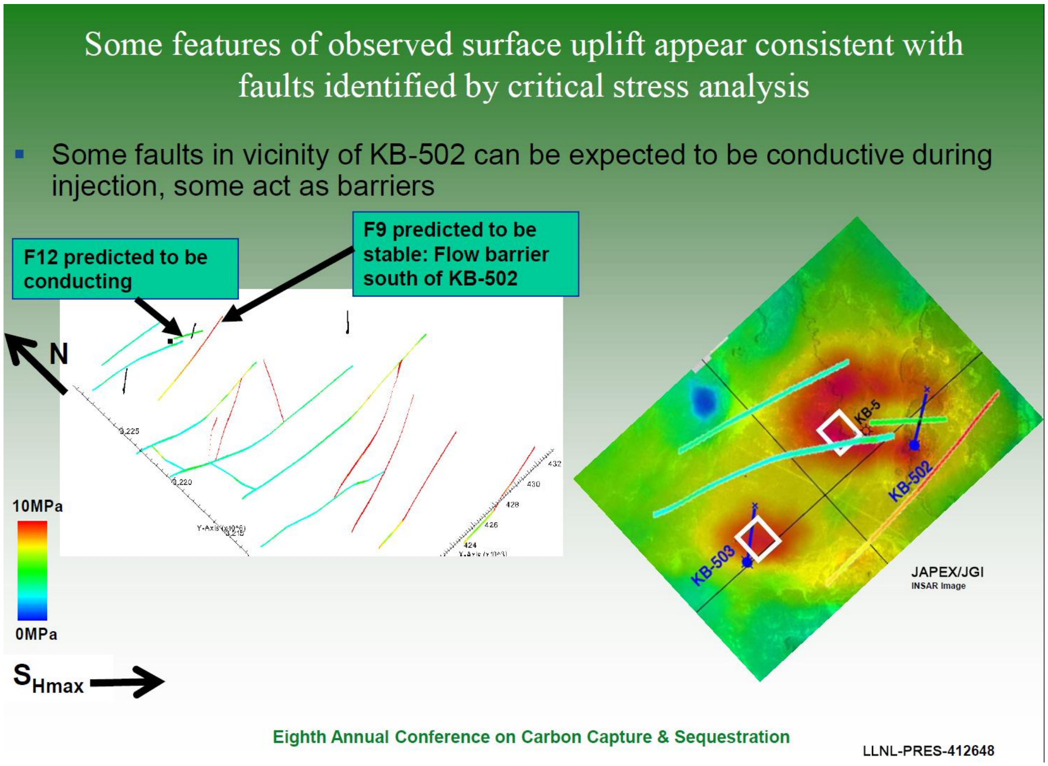
Some features of observed surface uplift appear consistent with faults identified by critical stress analysis
Some faults in vicinity of KB-502 can be expected to be conductive during injection, some act as barriers
F12 predicted to be conducting
F9 predicted to be stable: Flow barrier south of KB-502
N
10MPa
0MPa
S_{Hmax}
KB-5
KB-502
KB-503
JAPEX/JGI
INSAR Image
Eighth Annual Conference on Carbon Capture & Sequestration
LLNL-PRES-412648

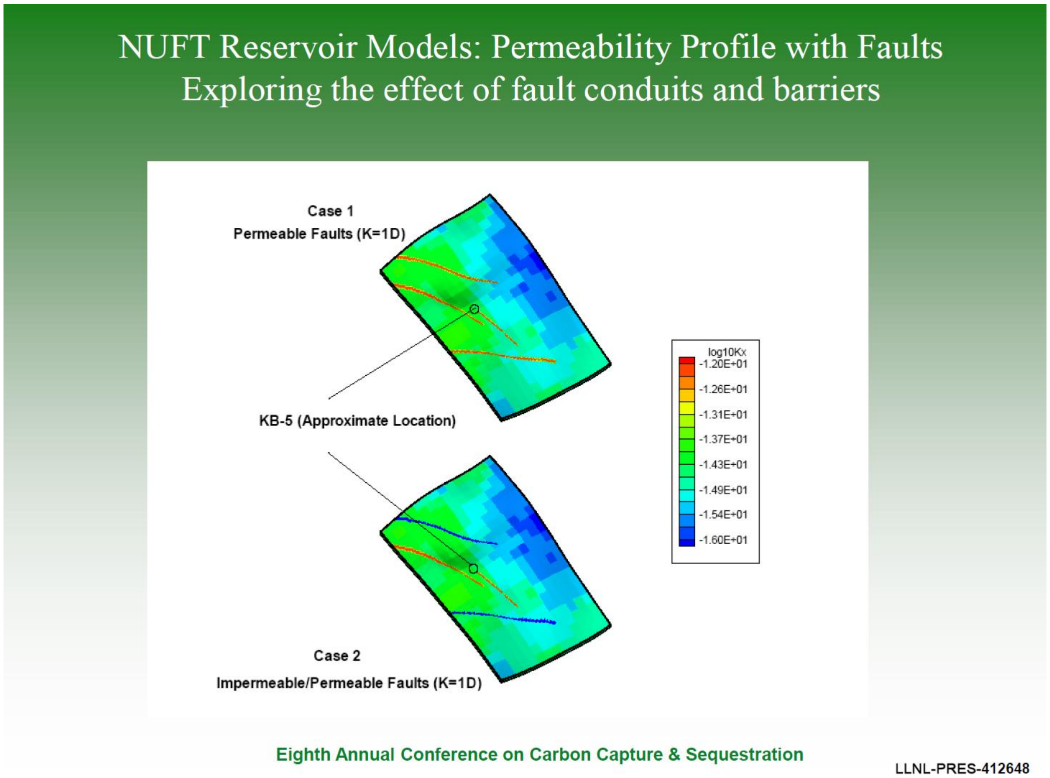
NUFT Reservoir Models: Permeability Profile with Faults
Exploring the effect of fault conduits and barriers
Case 1
Permeable Faults (K=1D)
KB-5 (Approximate Location)
Case 2
Impermeable/Permeable Faults (K=1D)
log10Kx
-1.20E+01
-1.26E+01
-1.31E+01
-1.37E+01
-1.43E+01
-1.49E+01
-1.54E+01
-1.60E+01
Eighth Annual Conference on Carbon Capture & Sequestration
LLNL-PRES-412648

Fault F12 provides a fast flow path: Observe early arrival at KB-5 well, consistent with observation

Case 1: Permeable Faults (K = 1 Darcy)

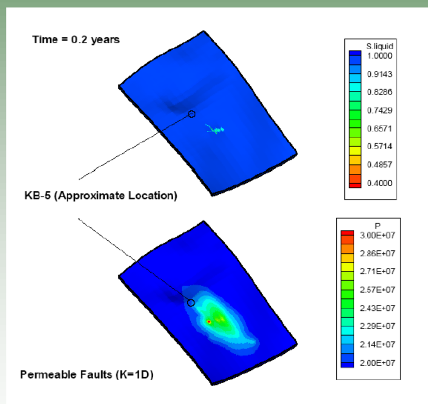

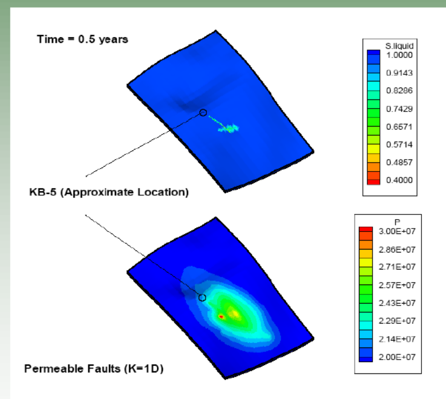

Eighth Annual Conference on Carbon Capture & Sequestration

LLNL-PRES-412648

Introduction of flow barriers leads to larger pressure perturbation

Case 1: Permeable Faults

Case 2: Impermeable/Permeable Faults

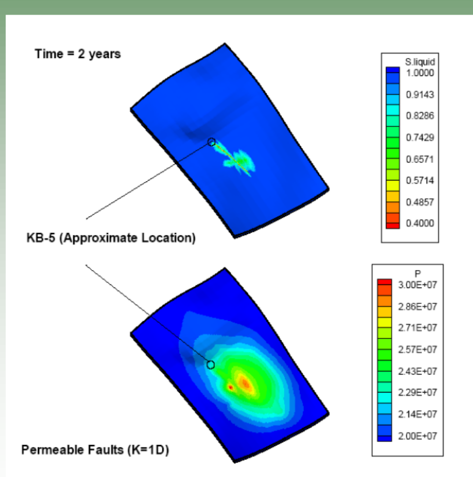

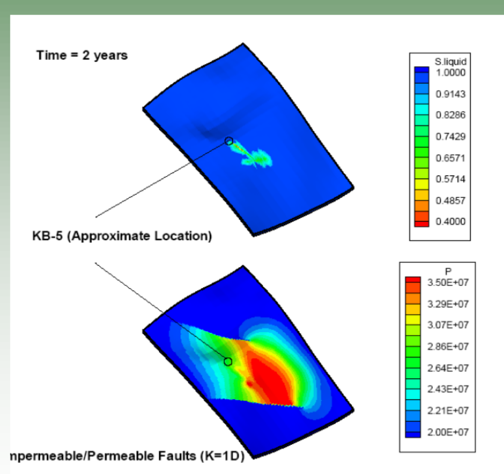

Eighth Annual Conference on Carbon Capture & Sequestration

LLNL-PRES-412648

Comparison with InSAR Data:
Magnitude of uplift is consistent with observation

Case 1: Permeable Faults

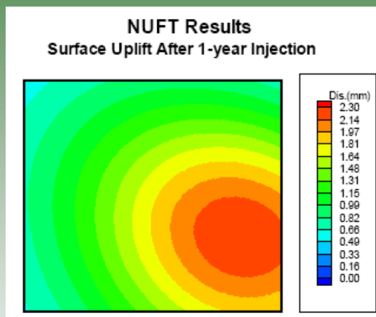

Case 2: Impermeable/Permeable Faults

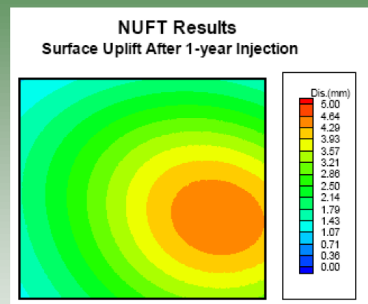

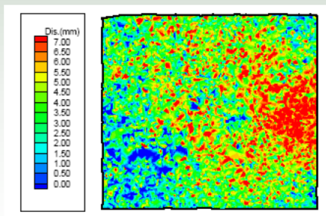

Surface Relative Displacement
(between 20050418 and 20060403)

LDEC – Livermore Distinct Element Code:
Explicitly includes mechanics of fracture network and faults

- Fault network in LDEC
  - Pre-injection stability predicted by LDEC matches critical stress analysis (as it should)

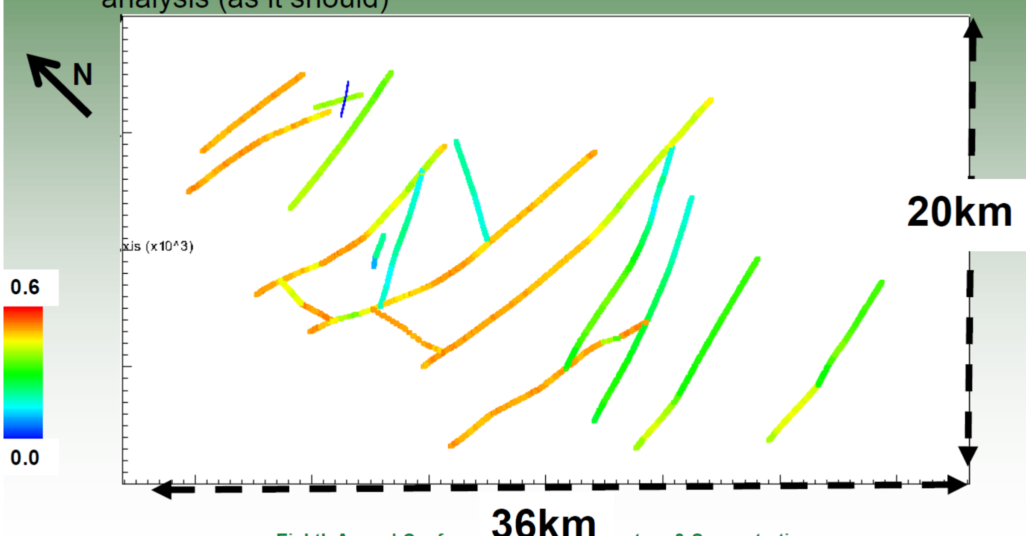

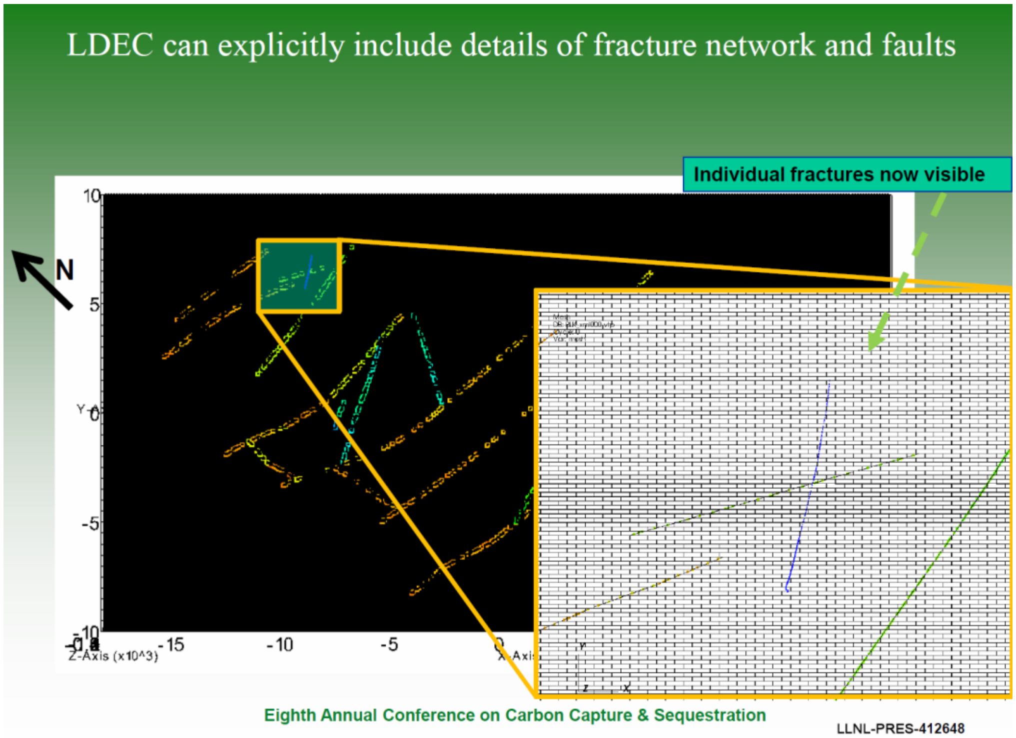
LDEC can explicitly include details of fracture network and faults
Individual fractures now visible
N
10
5
0
-5
-10
-15
-10
-5
Z-Axis (x10^3)
Eighth Annual Conference on Carbon Capture & Sequestration
LLNL-PRES-412648

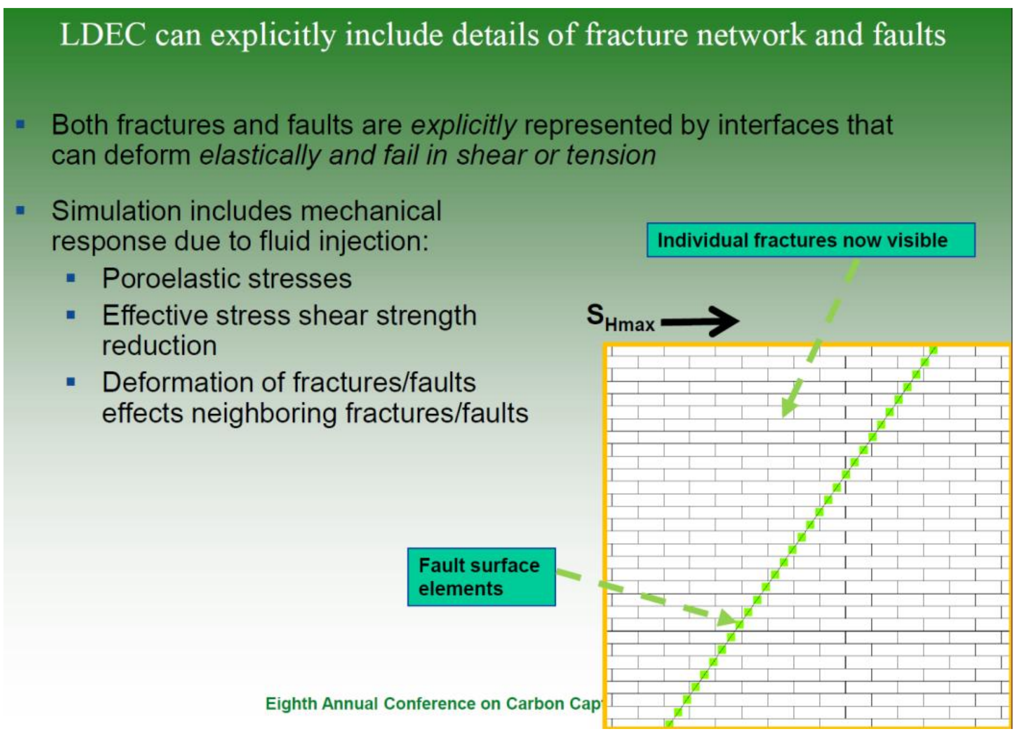
LDEC can explicitly include details of fracture network and faults
Both fractures and faults are *explicitly* represented by interfaces that can deform *elastically and fail in shear or tension*
Simulation includes mechanical response due to fluid injection:
Poroelastic stresses
Effective stress shear strength reduction
Deformation of fractures/faults effects neighboring fractures/faults
Individual fractures now visible
S_{Hmax}
Fault surface elements
Eighth Annual Conference on Carbon Cap

LDEC study of KB-502 area: Observe fault slip, but not fracture network Implies permeability enhancement isolated to faults

- "Baseline" candidate plume and stress orientation

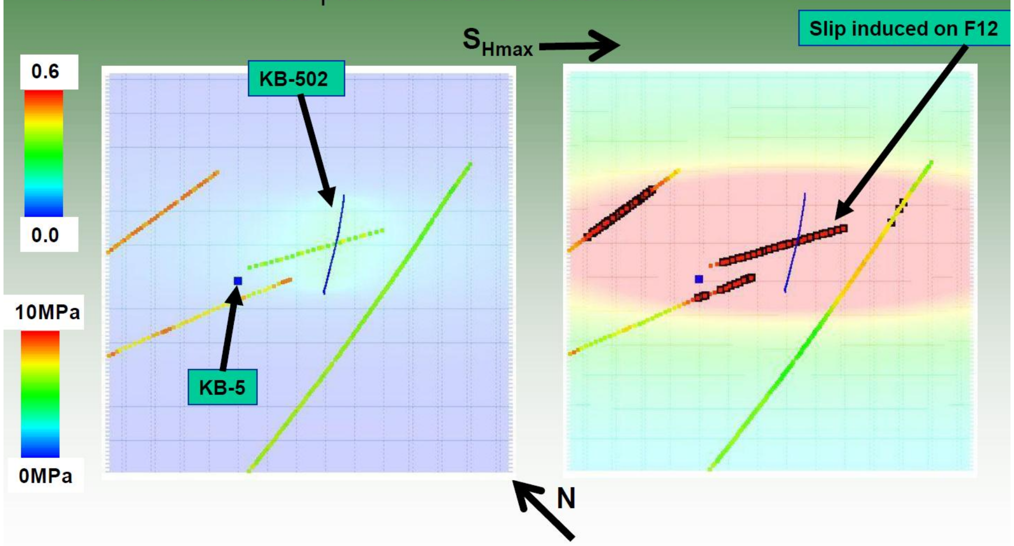

LDEC study of KB-502 area – Parameter study investigates role of combined in situ stress and fracture orientation

- Relative to the baseline case:
  - Explored effect of rotating in situ stress relative to fractures/faults
    - Intended to explore influence of:
      - Uncertainty of in situ stress orientation
      - Fracture strike variability
      - Fault strike uncertainty/variability
  - Varied plume geometry
    - The induced shear component associated with the poroelastic stresses vary with plume geometry
    - Different shaped plumes of same magnitude change in pore pressure induce different mechanical response

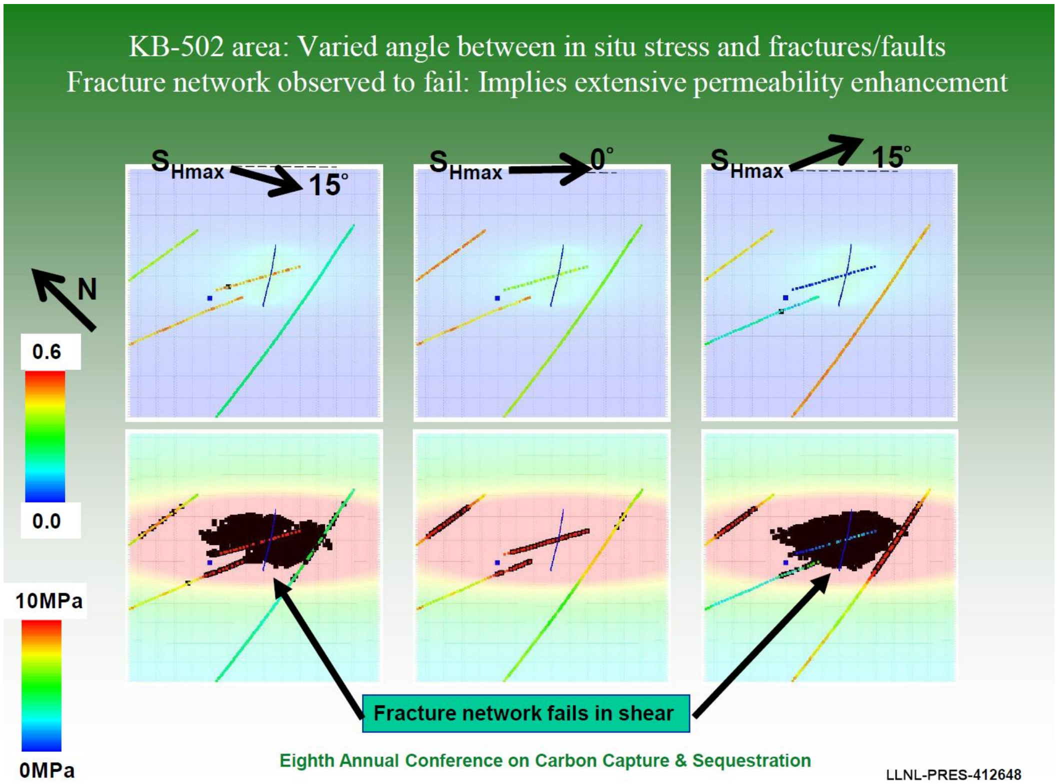
KB-502 area: Varied angle between in situ stress and fractures/faults
Fracture network observed to fail: Implies extensive permeability enhancement
SHmax 15°
SHmax 0°
SHmax 15°
N
0.6
0.0
10MPa
0MPa
Fracture network fails in shear
Eighth Annual Conference on Carbon Capture & Sequestration
LLNL-PRES-412648

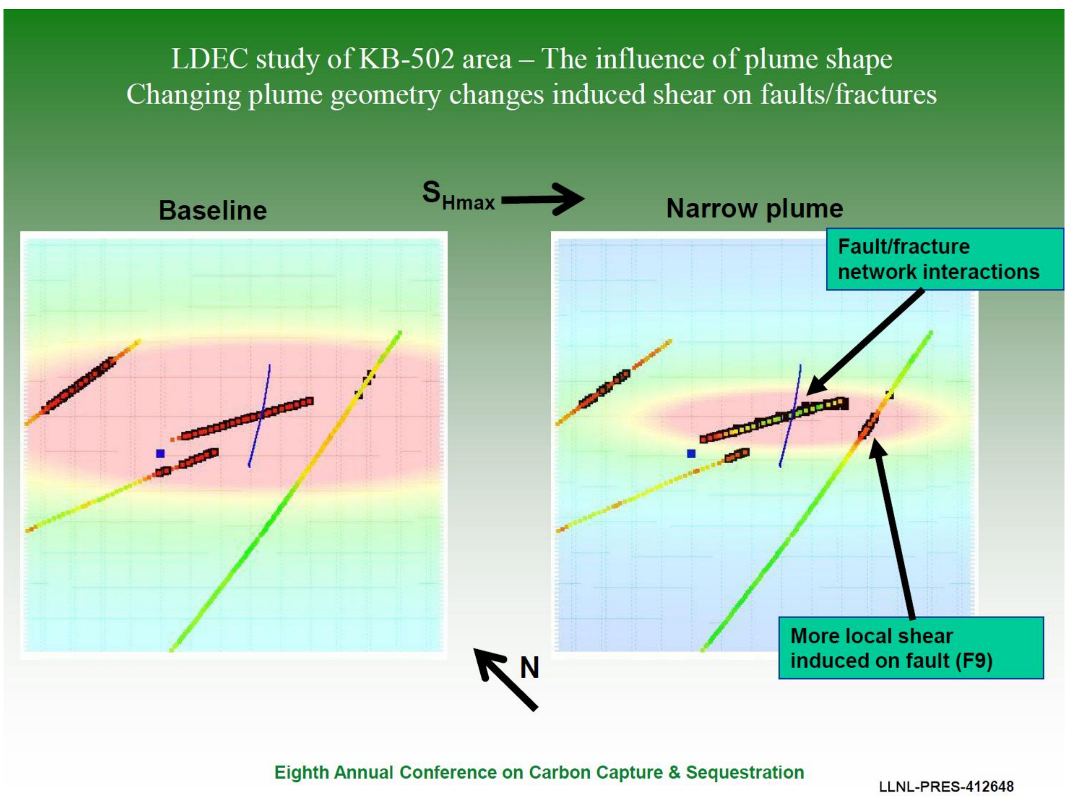
LDEC study of KB-502 area – The influence of plume shape
Changing plume geometry changes induced shear on faults/fractures
Baseline
SHmax
Narrow plume
Fault/fracture network interactions
More local shear induced on fault (F9)
N
Eighth Annual Conference on Carbon Capture & Sequestration
LLNL-PRES-412648

LDEC study of KB-502 area: Plume shape and in situ stress rotated 5°
Small changes in relative orientation lead to extensive permeability change

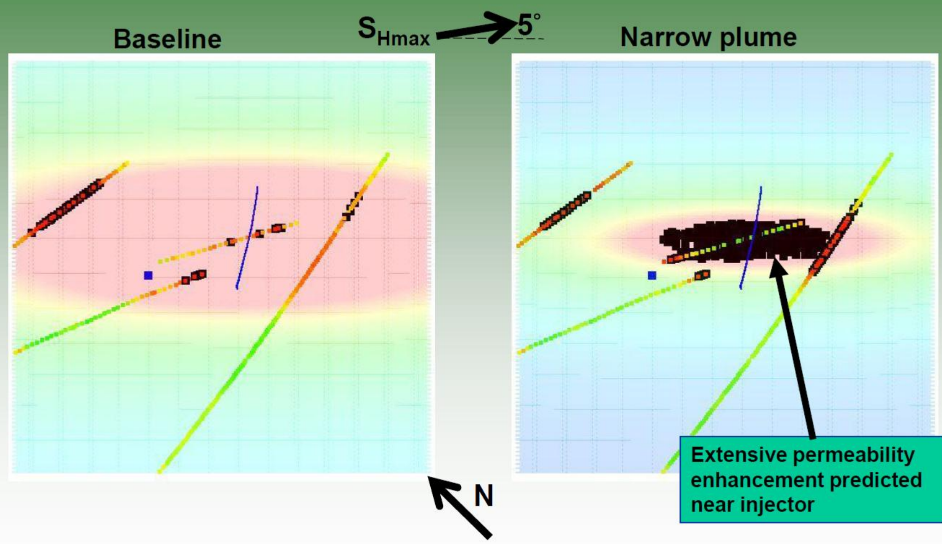

Eighth Annual Conference on Carbon Capture & Sequestration

LLNL-PRES-412648

Summary

- Faults in vicinity of KB-502 are expected to act as flow conduits and barriers
  - Consistent with observations
  - NUFT predicting magnitudes of uplift consistent with observation
- The degree of predicted permeability change is dependent upon:
  - Orientation of in situ stress relative to fractures
  - Plume shape
    - Controlled by reservoir heterogeneity, variable injectivity along injector, presence of conducting or impermeable faults
- Simulations have primarily focused upon the reservoir response:
  - Expect significant permeability enhancement due to shear response near injectors
  - Future work will consider the response of the overburden in more detail
- We have reports documenting this and geochemical studies in detail

Eighth Annual Conference on Carbon Capture & Sequestration

LLNL-PRES-412648

Acknowledgements

- Funding
  - JIP (a consortium of BP, StatoilHydro and Sonatrach)
  - DOE Fossil Energy

- Data was provided by the JIP.

- Special thanks to P. Ringrose (StatoilHydro) for the detailed geological models.

My email: morris50@llnl.gov

Eighth Annual Conference on Carbon Capture & Sequestration

LLNL-PRES-412648

ARMA 09-17

Coupled Hydromechanical and Reactive Transport Processes with Application to Carbon Sequestration

Morris, J. P., McNab, W. W., Johnson, S. M., Hao, Y.
Lawrence Livermore National Laboratory, Livermore, CA, U.S.A.

This paper was prepared for presentation at Asheville 2009, the 43rd US Rock Mechanics Symposium and 4th U.S.-Canada Rock Mechanics Symposium, held in Asheville, NC June 28th – July 1, 2009.

ABSTRACT: Large-scale carbon capture and storage (CCS) projects are the central infrastructural element needed to substantially reduce greenhouse gas emissions in a decarbonized fossil fuel energy system. Predicting the ultimate fate of the injected CO_2 involves understanding the interrelationship between multiple processes. These processes change the pore space within the reservoir, potentially modifying the permeability tensor within the reservoir. Furthermore, the flow in many target reservoirs is fracture dominated and fractures by nature can exaggerate the interrelationship between different processes. We present results of an ongoing study of the different processes at work within a fractured reservoir target for CO_2 storage.

1. INTRODUCTION

Large-scale carbon capture and storage (CCS) projects are the central infrastructural element needed to substantially reduce greenhouse gas emissions in a decarbonized fossil fuel energy system. Already, a number of industrial entities have announced large injection projects and plan to commence annual injection of millions of tons of CO_2 in the immediate future. Typically, this scenario involves injecting CO_2 into a porous, permeable formation that is overlain by an impermeable “caprock”.

Predicting the ultimate fate of the injected CO_2 involves understanding the interrelationship between multiple processes (see Fig. 1, Johnson et al. 2004). For example, the large rate and volume of injection will induce pressure and stress gradients within the formation that may activate existing fractures and faults, or drive new fractures through the caprock, creating new flow paths. In addition, reactions induced by the presence of CO_2 will result in modifications to the pore space within the reservoir, potentially modifying the permeability tensor within the reservoir. Furthermore, the flow in many target reservoirs is fracture dominated and fractures by nature can exaggerate the interrelationship between different processes. A small change in aperture, due to precipitation, may result in a large change in permeability. Similarly, relatively small changes in stress state may induce large changes in fracture permeability. Reactive flow may also dissolve material within previously cemented fractures, resulting in new flow paths for the CO_2.

We will present results of an ongoing study of the different processes at work within a fractured reservoir target for CO_2 storage. We will report results obtained with specialized computational tools to predict the hydromechanical coupling of fluid flow and stress within fracture networks. We will also discuss the implications these results have for the transport and ultimate fate of sequestered CO_2.

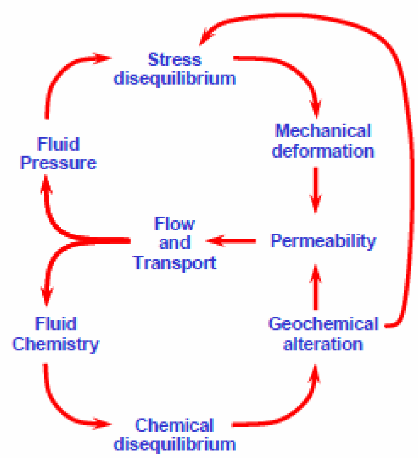

Fig. 1. Chemical, mechanical and flow properties are interdependent (depicted at left). In some cases, these effects may be in competition.

2. THE IN SALAH PROJECT: A FULL SCALE CO_2 SEQUESTRATION PROJECT

The In Salah Project (a joint venture of BP, StatoilHydro and Sonatrach) includes a CO_2 sequestration effort that has successfully injected millions of tons of CO_2 into a deep saline formation close to a producing gas field in Algeria. We have been jointly funded by the Joint Industry Project (A consortium consisting of BP, StatoilHydro and Sonatrach, hereafter referred to as the JIP) and the U.S. Department of Energy to investigate the role of injection induced mechanical deformation and geochemical alteration at the In Salah CO_2 storage project. In this paper we will focus upon the hydromechanical portion of this study. More details can be found in Morris et al., 2009.

2.1. Simulations of hydromechanical response of individual fractures

We have performed analyses of the influence of pore pressure on fractures in the vicinity of one of the injectors using Frac-HMC (Detwiler et al., 2006). This analysis predicts the evolution of permeability in response to normal displacement changes resulting from increases in pore pressure (see Figure 2) including details of aperture distribution within the fracture. We constructed a model of a fracture within the reservoir based upon data provided by the JIP. The Frac-HMC simulation calculated the change in aperture distribution throughout the fracture and associated permeability increase in response to increases in pore pressure. The results (see Figure 2) indicate significant permeability increase is to be expected.

2.2. Simulations of hydromechanical response of extensive fracture networks and intersecting faults

The previous section discussed the response of individual fractures to fluid injection. We have commenced modeling the response of extensive fracture networks, including detailed intersections with faults. This work to date has considered only fractures and faults within the reservoir itself. These faults have not been observed to persist into the overburden. Consequently, this initial study is concerned only with predicting the evolution of permeability in the reservoir and not the caprock response.

Our first studies consisted of critical stress analysis (similar to Chiaramonte et al., 2006) to determine which faults are expected to act as fast flow paths and which will be flow barriers. Figure 3 shows our prediction of propensity for shear on the faults. The color scale reflects the magnitude of pore-pressure change required to induce slip on the segments of the faults. Consequently, it can be seen that several faults are critically stressed and likely to provide fast flow paths. This analysis identified several faults in the vicinity of one of the injectors that may be responsible for features observed in the surface deformation (see Fig. 4). Specifically, the uplift observed above the KB-502 injector is consistent with the nearby “F9” fault acting as a flow barrier.

Further hydromechanical studies were conducted by incorporating the fault model into a combined fracture network-fault network representation using the LDEC code (Morris et al., 2003). LDEC is capable of simulating extensive combined fracture fault network response to pore pressure perturbation (Morris et al., 2008).

Figure 5 highlights that in addition to the details of the faults, the response of the fractures is also included in the LDEC model. Figure 6 shows the response of the combined fracture and fault network to a hypothetical pore pressure increase as part of a parameter study (see Morris et al., 2009 for more details). These calculations consider the poroelastic response of the fractured rockmass and include the redistribution of stresses through the combined fracture-fault network. The black regions highlight sections of the faults and fractures that fail and will provide enhanced permeability within the reservoir. We explored the effect of rotating the in situ stress relative to fractures/faults. This was intended to explore influence of uncertainty of in situ stress orientation, fracture strike variability and fault strike uncertainty/variability.

The results of these studies indicate that significant permeability evolution is expected within the reservoir due to combinations of fracture and fault deformation. One key observation is that the fracture network and in situ stress are oriented in such a way that the extent of permeability evolution is very sensitive to the orientation of the in situ stress field. In short, the shape and extent of the plume is predicted to be highly sensitive to small variations in the relative orientation to the in situ stress.

In the future, this model will be iteratively coupled with reservoir scale reactive transport modeling to investigate the interaction between mechanical and geochemical processes.

2.3. Reactive Transport Studies

Our geochemical reactive transport simulation effort has been divided into two subtasks: (1) multiphase flow simulation of CO_2 injection into the Krechba field, and (2) simulation of water-rock interactions involving mineral phases present in the cap rock and reservoir and reservoir water equilibrated with supercritical CO_2 at ambient pressure and temperature conditions. In this paper we discuss the second component of this investigation.

Using data provided by the JIP, we have developed a 2-D reactive transport model for reactive single-phase flow through a 10-m x 10-m block of fractured reservoir material containing simulated distributions of relevant mineral phases. Specifically, the model entailed using the U.S. Geological Survey's PHAST code to model the flow of water, equilibrated with supercritical CO2 at 95°C and 200 bars, through preferential flow pathways that result from local variability in fracture aperture. Initial spatial distributions of the mineral phases as well as fracture aperture (and hence hydraulic conductivity via the cubic law) were created using a random spatially-correlated Gaussian field generator (Fig. 7). The goal of the reactive transport modeling is to assess the sensitivity of model predictions to various assumptions concerning reaction rates of key mineral phases (Fig. 8). The reactive transport modeling effort is ongoing and will ultimately be used to quantify the dynamic response of the permeability field as a result of mineral precipitation and dissolution reactions for larger-scale simulations of CO2 injection at the Krechba field. The preliminary conclusion is that although changes in porosity are predicted, the magnitude of the changes is insufficient to have a significant impact upon the permeability of fractures or faults in the reservoir or the caprock.

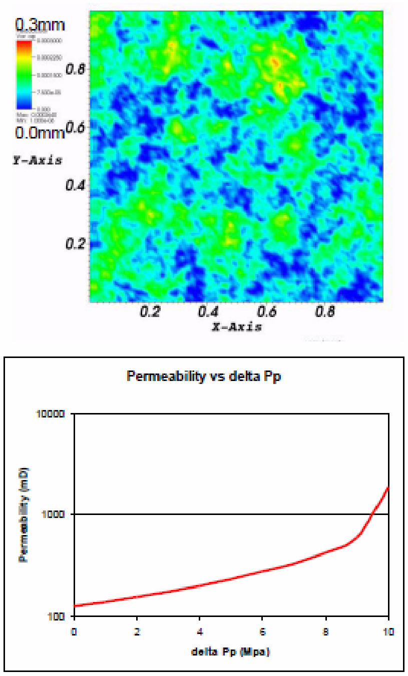

Fig. 2. Top: Aperture distribution within Frac-HMC representation of a single fracture. Bottom: Frac-HMC prediction of permeability evolution with increasing pore pressure. An order of magnitude increase in permeability is predicted for as the pore pressure increases by 10 MPa.

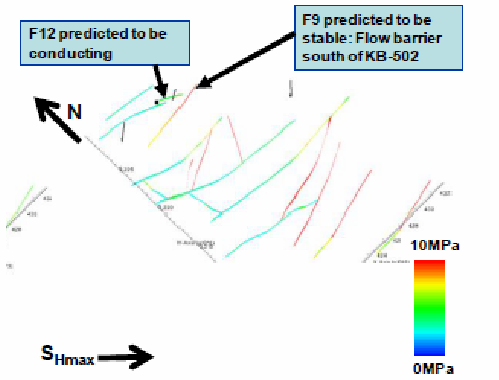

Fig. 3. We performed critical stress analysis of a preliminary fault model for the Krechba reservoir. These faults are within the reservoir itself and do not persist into the overburden.

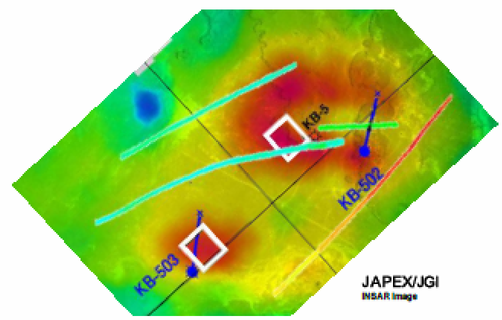

Fig. 4. Direct comparison of fault stability analysis (from Fig. 3) with observed uplift on InSAR. The uplift (yellow and red) associated with KB-502 injection appears consistent with F9 acting as a flow barrier

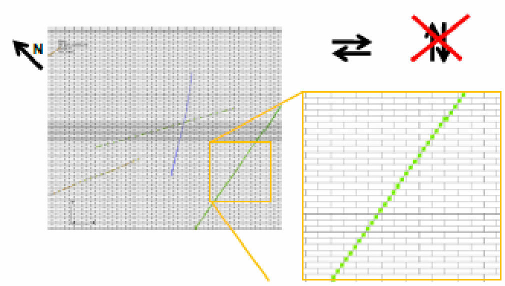

Fig. 5. Preliminary fault model for the Krechba reservoir built within LDEC, highlighting the details of the individual fractures within the network. The model includes 400,000 individual fracture elements.

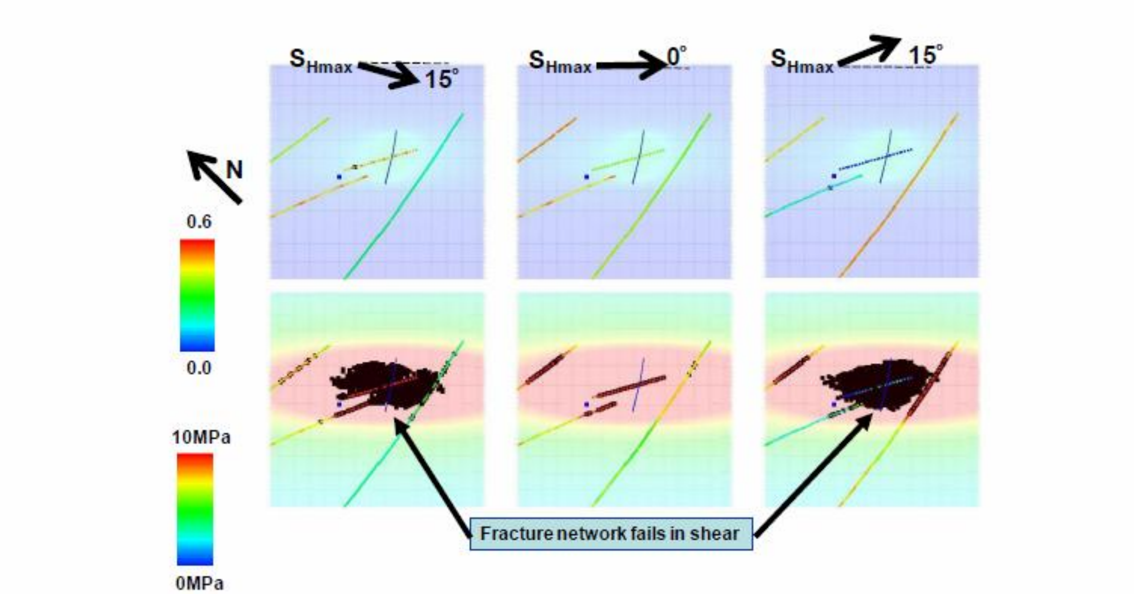

Fig. 6. In response to injection, portions of the faults and fractures experience shear slip depending upon the precise orientation of the in situ stress field. This implies that extensive permeability enhancement may be expected dependent upon the conditions in the field.

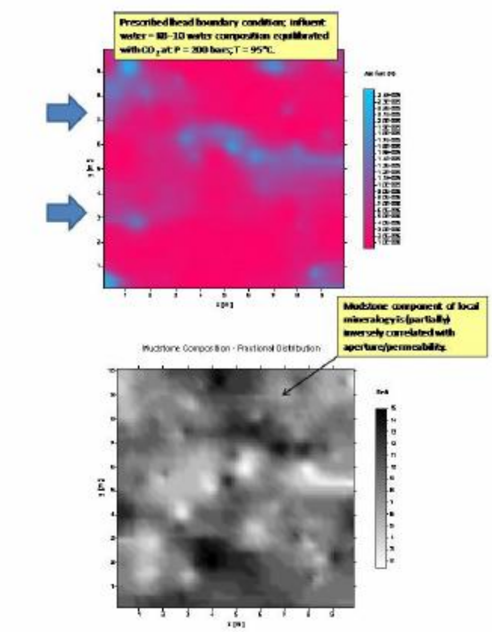

Fig. 7. Random aperture field across the simulated fracture used to calculate local permeability (top) and corresponding distribution of clay-rich mudstone component (bottom). The darker color portions of the lower figure correspond to regions containing up to a 70% mudstone fraction; lighter color regions consist primarily of quartz with only trace amounts of mudstone.

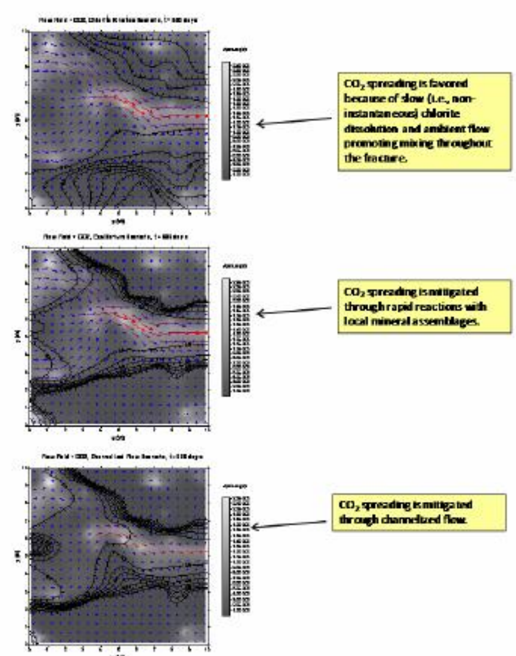

Fig. 8. Distribution of CO_2 after 500 days under three different sets of assumptions: kinetically-controlled chlorite dissolution under baseline flow conditions (top), rapid dissolution under baseline flow conditions (middle), and kinetically-controlled dissolution under channeled flow conditions (bottom). Lateral spreading of CO_2 is limited in the second case by water-rock interactions and in the third (bottom) case by restricted flow.

ACKNOWLEDGEMENTS

This work was conducted with the support of the JIP (a consortium of BP, StatoilHydro and Sonatrach) and DOE Fossil Energy under the auspices of the U.S. Department of Energy by Lawrence Livermore National Laboratory under Contract DE-AC52-07NA27344. Data was provided by the JIP. The author wishes to thank P. Ringrose (StatoilHydro) for the detailed geological models.

REFERENCES

1. Chiaramonte, L., M.D. Zoback, S.J. Friedmann, and V. Stamp, CO2 Sequestration, Fault Stability and Seal Integrity at Teapot Dome, Wyoming, NETL 5th Annual Conference on Carbon Sequestration, Alexandria, VA, Exchange Monitor Publications, 2006.
2. Detwiler, R.L., J.P. Morris and S.M. Ezzedine, Coupling micromechanics and fluid flow through discrete fracture networks: Quantifying effective permeability under variable stress conditions, Eos Transactions AGU, 86(46), Fall Meeting Supplement, Abstract H13D-1433,2006.
3. Johnson, J.W., J.J. Nitao, J.P. Morris, 2004, "Reactive Transport Modeling of Cap Rock Integrity During Natural and Engineered CO2 Storage," in Carbon Dioxide Capture for Storage in Deep Geologic Formations (Elsevier: ISBN0080445705)
4. Morris, J.P., M. B. Rubin, S. C. Blair, L. A. Glenn and F. E. Heuze, Simulations of Underground Structures Subjected to Dynamic Loading using the Distinct Element Method, Engineering Computations, Vol. 21 (2/3/4), 384-408, 2003.
5. Morris, J.P., S. Johnson, S.J. Friedmann, 2008, "Geomechanical Simulations of Caprock Integrity using the Livermore Distinct Element Method," 7th Annual Conference on Carbon Capture & Sequestration, Pittsburgh, Pennsylvania.
6. Morris, JP, Carroll S.A., Mcnab, W.W., Hao, Y., Foxall, W.F, Ramirez, A.L., Quarterly Report for Injection and Reservoir Hazard Management: The Role of Injection-Induced Mechanical Deformation and Geochemical Alteration at In Salah CO2 Storage Project, LLNL-TR-412713, March 2009.

Article submitted to GEOSTRATA:

CO_2 sequestration: Fracture properties will control storage performance

Authors: Joseph Morris, morris50@llnl.gov and
Laura Pyrak-Nolte, ljpn@physics.purdue.edu

We present results from an ongoing computational study of the In Salah Gas CO_2 Storage Project. This project involves injection of approximately one million tons of CO_2 per annum into a deep saline formation in Algeria. Our evolving understanding of the response of the reservoir illustrates how fractures act to amplify the coupling between chemical and hydromechanical processes. This sequestration project is merely one example of what will ultimately be many projects that are needed to achieve significant reductions in greenhouse gas emissions. Although each future project will involve distinct geological features, many will include geologic targets containing preexisting fractures. In addition, the large rate and volume of injection may induce pressure perturbations within the formation that can activate existing fractures and faults, or create new fractures within the reservoir or caprock. Consequently, understanding the role of fractures in controlling flow through rock masses is key in predicting the performance of industrial-scale CO_2 geological storage.

In Salah Gas (ISG) is a joint venture of BP, Sonatrach, and StatoilHydro that has two fundamental goals: (1) 25-30 years of 9 bcfy natural gas production from 8 fields in the Algerian Central Sahara, and (2) successful minimization of the associated environmental footprint by capture and subsurface isolation of the excess CO_2 extracted from production streams. The gas produced from these fields is too rich in CO_2 for export to Europe and consequently is purified before being piped out of the field area. Figure 1 shows a photograph of the surface facilities associated with the CO_2 removal process. In previous analogous operations, the separated CO_2 has been vented, but at In Salah since 2004, the CO_2 has been stored in a deep saline formation, down-dip from the producing gas field (see Figure 2).

Predicting the hydromechanical response of the reservoir at Krechba is proving important in order to understand the ultimate fate of the injected CO_2. Specifically, although there is no evidence of faulting through the caprock, there are faults and extensive fracture networks within the reservoir itself that potentially control the mobility of the CO_2. Figure 3 shows the current map of the potential faults identified within the reservoir and also shows some of the fractures identified from FMI logs. Recent hydromechanical analysis performed by Lawrence Livermore National Laboratory (LLNL) under funding from the In Salah Gas Storage Joint Industry Project (JIP, a consortium of BP, StatoilHydro and Sonatrach) and the U.S. Department of Energy has demonstrated that features of the fault map are consistent with observation of surface uplift and detection of CO_2 by monitoring wells (see Figure 4; Morris et al., CCS Conference, Pittsburgh, 2009).

LLNL performed additional analysis to investigate deformation of the fracture network within the reservoir (see Figure 5; Morris et al., CCS Conference, Pittsburgh, 2009). Fractures that fail in shear are expected to develop enhanced permeability, resulting in modification of the CO_2 plume. Figure 5 shows the response of the combined fracture and fault network to a hypothetical pore pressure increase under different in situ stress conditions. This calculation considers the poroelastic response of the fractured rockmass and includes the redistribution of stresses through the combined fracture-fault network. The black regions highlight sections of the faults and fracture network that fail and will provide enhanced permeability within the reservoir. In particular there are two fault sections near the injection site that are predicted to be conduits for fast flow in this scenario. Uncertainty in situ stress orientation, fracture strike variability and fault strike uncertainty/variability was also explored. It is observed that the fracture network is very sensitive to the orientation of the in situ stress.

In addition to hydromechanical effects, injection of CO_2 into a subsurface reservoir can initiate a complex set of geochemical reactions that involve interactions between aqueous solutions and the minerals in the host rock (see Figure 6). These reactions can lead to mineral precipitation in voids and fractures or dissolution of the host rock. The hydro-mechanical behavior of fractures can be significantly affected by such geochemical interactions. For example, while dissolution of fracture surfaces may initially enlarge the apertures in a fracture, the subsequent changes in the stress distribution along the fracture plane can lead to closure or reductions in apertures that in turn reduced fluid flow through the fracture. Recent laboratory experiments have shown that preferential dissolution at points of contact between surfaces can lead to large displacements that rapidly reduce fracture apertures. The amount and rate of closure of a fracture subjected to dissolution depends on the spatial distribution of apertures within the fracture which controls the hydrodynamic behavior and also on the spatial distribution of local chemical reaction rates. On the other hand, mineral precipitation within a fracture can lead to blocking or plugging of the fracture thereby reducing storage capacity of a reservoir or potentially acting as a mineral seal to trap CO_2 in the subsurface.

Acknowledgements

This work was conducted with the support of the ISG CO_2 JIP (a consortium of BP, StatoilHydro and Sonatrach) and DOE Fossil Energy under the auspices of the U.S. Department of Energy by Lawrence Livermore National Laboratory under Contract DE-AC52-07NA27344.

Figure 1: The amine CO_2 removal facilities at Krechba. This facility removes CO_2 from the production streams of several reservoirs to render the product suitable for export to Europe. Separated CO_2 is normally vented from such gas plants, but at In Salah, the separated CO_2 is geologically stored in a deep saline formation that has been characterized to oil and gas standards. (Image courtesy Iain Wright, BP)

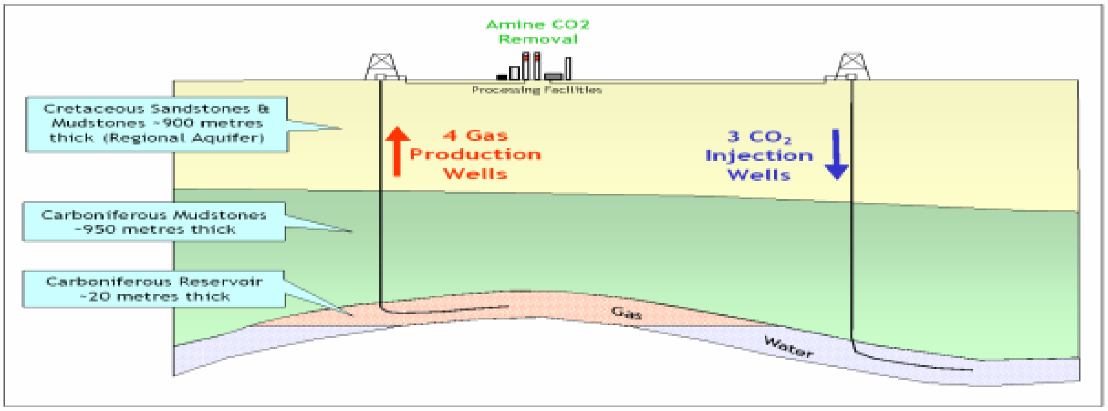

Figure 2: Depiction of the injection scenario employed at Krechba. CO_2 is removed from the gas streams of multiple production reservoirs and is reinjected into the Krechba Carboniferous sandstone reservoir at a depth of almost 2km. If this image were truly to scale, the 20 m thick reservoir would appear as a single, almost flat, line. (Image courtesy Phil Ringrose, StatoilHydro).

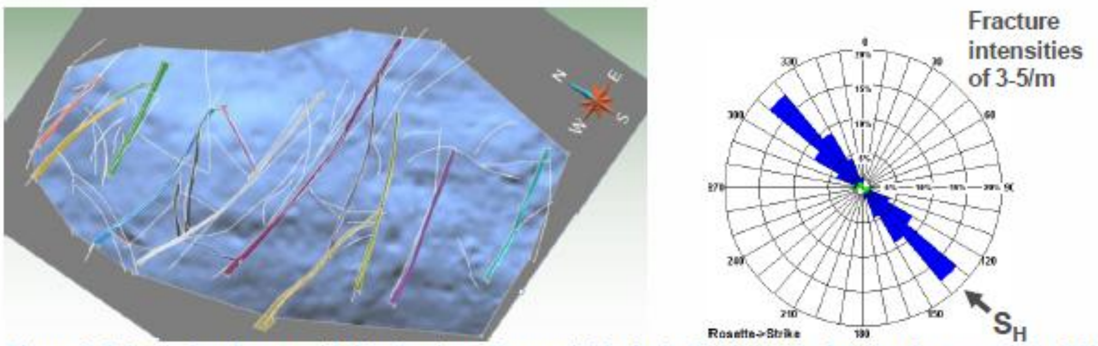

Figure 3: Seismic data has provided indications of potential faults in the reservoir, but not the caprock (at left). Observations of breakouts on FMI logs provide insight into the predominant fracture orientations (at right). (Data courtesy Phil Ringrose, StatoilHydro).

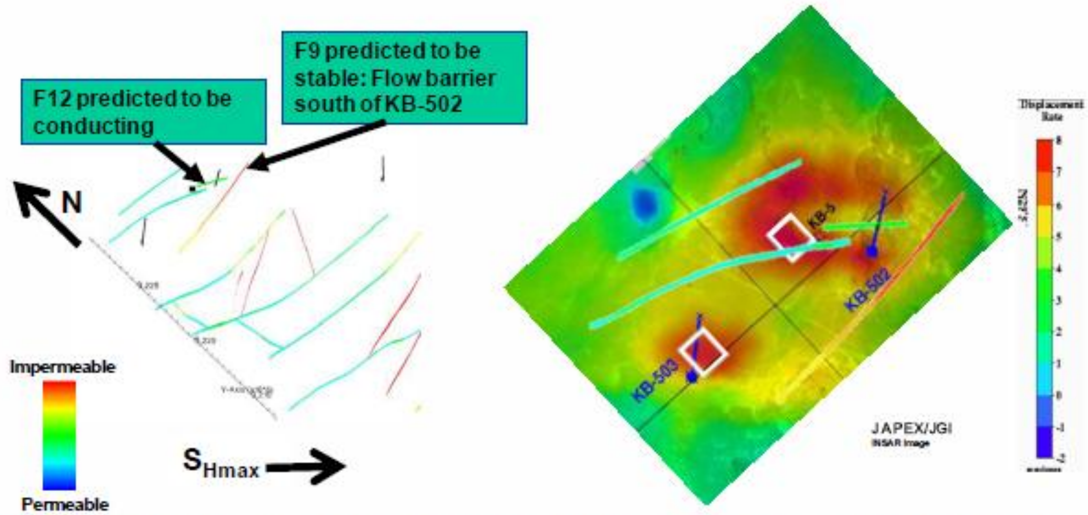

Figure 4: Geomechanical analysis of the fault system (at left) indicates faults which are expected to be fast flow paths (blue) and those which will perform as flow barriers (red). InSAR data (Onuma and Ohkawa, 2008, at right, with fault analysis overlaid) provides a remote sensing tool for monitoring volume change in the subsurface (red corresponds to uplift, and blue subsidence). It is observed that the surface displacement is consistent with the prediction that fault F9 acts as a flow barrier. Additionally, CO_2 has been detected at KB-5, consistent with F12 acting as a conductive feature.

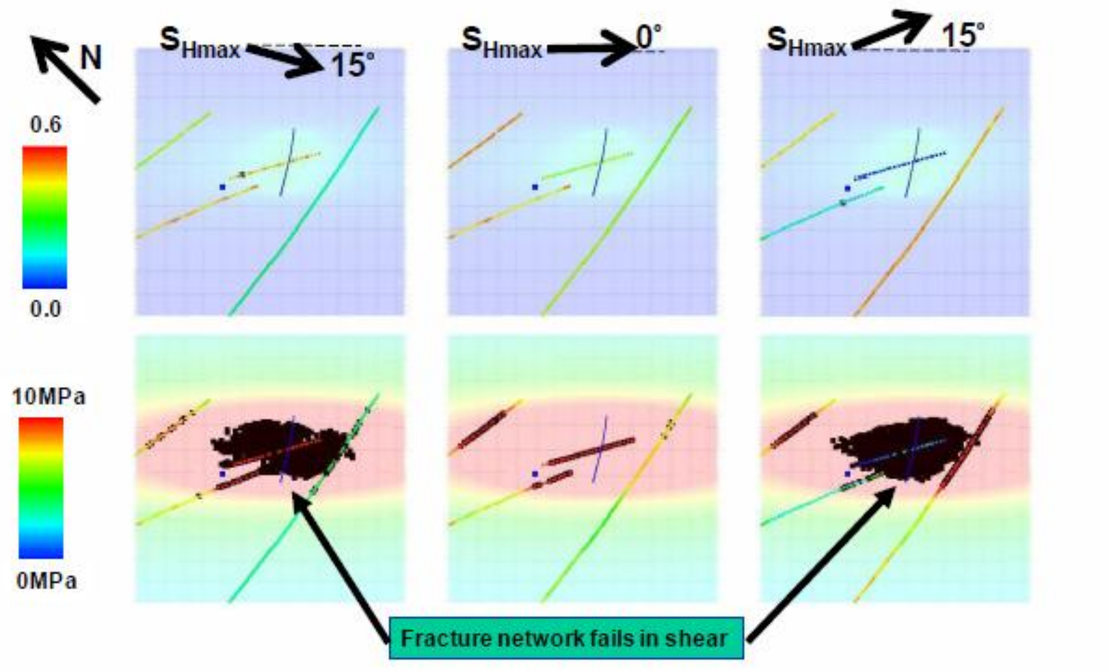

Figure 5: Discrete Element Simulations using the Livermore Distinct Element code for eXport (software licensed by LLNL) are exploring the sensitivity of the pore-pressure induced fracture network shear failure to uncertainty in the in situ stress orientation.

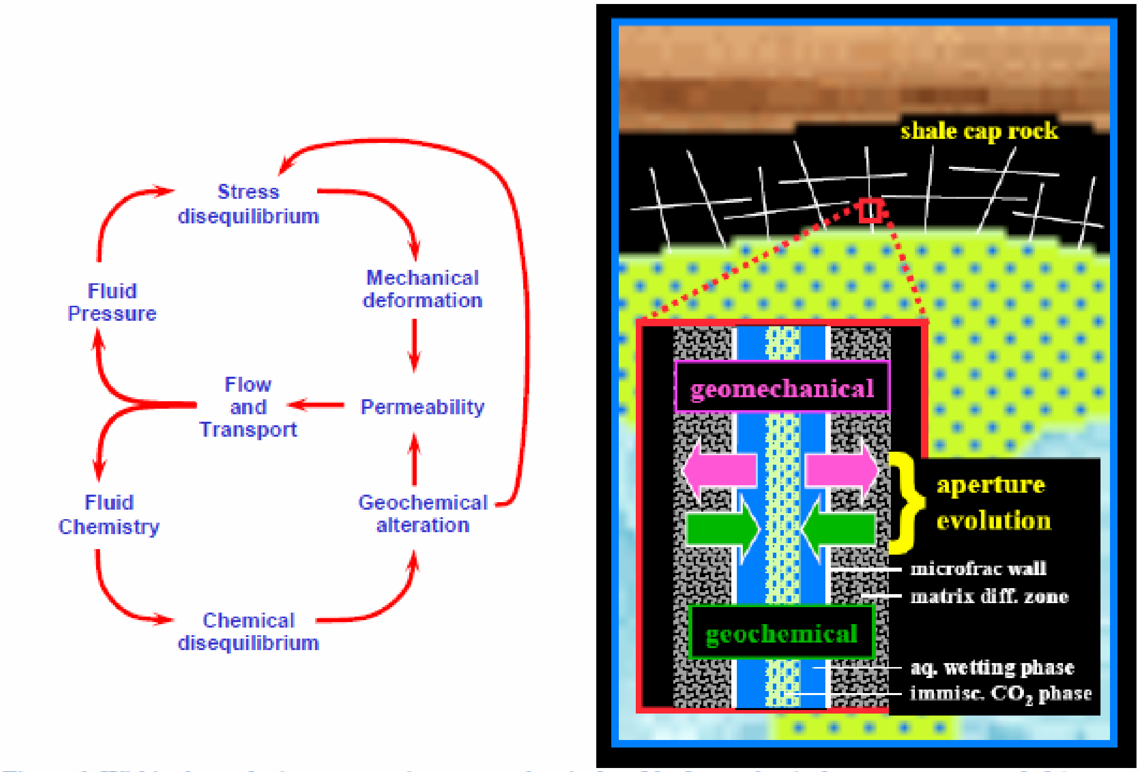

Figure 6: Within the geologic sequestration target, chemical and hydromechanical processes are coupled (at left). Fractures by their nature act to exaggerate such couplings (at right; Johnson et al., 2003). Specifically, small changes in aperture induced by chemical processes can result in large changes in the effective permeability.